

Research and Development at DWD

ICON Database Reference Manual

Version 1.1.9

Last changes: September 27, 2016

D. Reinert, F. Prill, H. Frank, and G. Zängl



Version: 1.1.9

This document is based on Revision 29378 of the ICON code, last changed on 2016-09-27.

DOI: 10.5676/DWD_pub/nwv/icon_1.1.9



The CC license “BY-NC-ND” allows others only to download the publication and share it with others as long as they credit the publication, but they can’t change it in any way or use it commercially.

Publisher

Deutscher Wetterdienst
Business Area “Research and Development”
Frankfurter Straße 135
63067 Offenbach
www.dwd.de

Editors

Daniel Reinert, FE13,
Tel. +49 (69) 8062-2060, daniel.reinert@dwd.de
Helmut Frank, FE13,
Tel. +49 (69) 8062-2742, helmut.frank@dwd.de
Florian Prill, FE13,
Tel. +49 (69) 8062-2727, florian.prill@dwd.de

Revision History

| Revision | Date | Author(s) | Description |
|----------|----------|-----------|--|
| 0.1.0 | 10.01.13 | DR, FP | Generated preliminary list of available GRIB2 output fields |
| 0.2.0 | 12.07.13 | DR, FP | Added a short section describing the horizontal ICON grid. AUMFL_S , AVMFL_S added to the list of available output fields |
| 0.2.1 | 15.07.13 | DR | Provide newly available output fields in tabulated form. Change levelType of 3D atmospheric fields from 105 (Hybrid) to 150 (Generalized vertical height coordinate) |
| 0.2.2 | 16.07.13 | FP | Short description of ICON's vertical grid. |
| 0.2.3 | 25.09.13 | DR | Added description of available First Guess and analysis fields |
| 0.2.4 | 17.12.13 | DR | Added description of external parameter fields |
| 0.3.0 | 24.01.14 | DR | Added information about horizontal output grids |
| 0.3.1 | 24.01.14 | DR | Added information about newly available output field OMEGA |
| 0.4.0 | 22.05.14 | HF | Added SKY-database documentation |
| 0.4.1 | 15.07.14 | DR | Some documentation on statistical processing and minor updates. New output fields ASWDIR_S , ASWDIFD_S , ASWDIFU_S , DTKE_CON |
| 0.4.2 | 10.09.14 | DR | New output fields CLCT_MOD , CLDEPTH |
| 0.5.0 | 01.10.14 | DR | Description of IAU initialization method |
| 0.5.1 | 15.10.14 | DR | Updated description of necessary input fields |
| 0.5.2 | 31.10.14 | DR | Add full table with model half level heights |
| 0.6.0 | 05.12.14 | DR | Add short introduction and fix some minor bugs |
| 0.6.1 | 10.12.14 | DR | New output field APAB_S |
| 0.7.0 | 16.12.14 | DR | Revised documentation of time invariant fields and a couple of bug fixes |
| 0.7.2 | 09.01.15 | DR | General GRIB2 description |
| 0.8.0 | 15.01.15 | FP, DR | Couple of bug fixes regarding the available fields on triangular and regular grids |
| 0.8.1 | 16.01.15 | FP, DR | List of pressure-level variables available on triangular grids |
| 0.8.2 | 16.01.15 | FP | List of height-level variables available on regular grids |
| 0.8.3 | 16.01.15 | DR | List of variables exclusively available for $VV = 0$ |
| 0.8.4 | 06.02.15 | FP, DR | Details of internal interpolation onto lon-lat grids. Details regarding output frequency. |
| 0.8.5 | 18.02.15 | FP | Additional pressure levels for regular grid output. |
| 0.8.6 | 23.02.15 | FP | Formula for computing non-zero topography level height. |
| 1.0.0 | 23.02.15 | FP | Additional table of model full levels. |
| 1.0.1 | 24.02.15 | DR | Update on available forecast runs and time span. |

Revision History

| | | | |
|-------|----------|--------|--|
| 1.0.2 | 27.02.15 | FP | Added tables for grid point with maximum topo height. |
| 1.0.3 | 13.03.15 | DR, FP | Section on statistically processed fields. |
| 1.1.0 | 15.04.15 | FP, DR | Section on ICON EU nest (preliminary). |
| 1.1.1 | 07.07.15 | HF | Added SMA list, list of half levels for EU nest, modified output lists to automatically write model level variables in the namelist templates. |
| 1.1.1 | 17.07.15 | HF | Preliminary add T_S because it is already written in operations. Some other minor modifications. |
| 1.1.2 | 14.08.15 | FP | Added note on ICON's earth radius and a table summarizing regular grids. |
| 1.1.3 | 04.12.15 | FP | Added WW code table 6.8 . |
| 1.1.4 | 11.01.16 | HF | Updated examples how to retrieve ICON data from SKY. |
| 1.1.5 | 22.01.16 | AR | Description of En-Var. |
| 1.1.6 | 28.01.16 | DR | Extend tables by field specific lat-lon interpolation method. |
| 1.1.7 | 11.04.16 | DR, FP | Add timeline of model changes. |
| 1.1.8 | 06.07.16 | HF | Add DTKE_HSH and other minor corrections. |
| 1.1.9 | 27.09.16 | DR | Update intro and timeline. |

Simulations are believed by no one except those who conducted them.

Experimental results are believed by everyone except those who conducted them.

ANONYMOUS

Contents

| | |
|--|-----------|
| 1. Introduction | 1 |
| 2. History of model changes | 3 |
| 3. Grid geometry | 5 |
| 3.1. Horizontal grid | 5 |
| 3.2. Vertical grid | 7 |
| 3.3. Refined subregion over Europe (“local nest”) | 7 |
| 4. Mandatory input fields | 11 |
| 4.1. Grid Files | 11 |
| 4.2. External parameters | 11 |
| 5. Analysis fields | 15 |
| 5.1. Ensemble Data Assimilation | 17 |
| 5.2. Incremental analysis update | 19 |
| 6. Global output fields: Forecast runs | 21 |
| 6.1. Deprecated output fields | 21 |
| 6.2. New output fields | 21 |
| 6.3. Available output fields | 22 |
| 6.3.1. Time-constant (external parameter) fields | 24 |
| 6.3.2. Multi-level fields on native hybrid vertical levels | 27 |
| 6.3.3. Multi-level fields interpolated to pressure levels | 28 |
| 6.3.4. Single-level fields | 30 |
| 6.3.5. Soil-specific multi-level fields | 34 |
| 6.3.6. Lake-specific single-level fields | 35 |
| 7. EU Nest output fields: Forecast runs | 37 |
| 7.1. Available output fields | 37 |
| 7.1.1. Time-constant (external parameter) fields for the EU nest | 38 |
| 7.1.2. Multi-level fields on native hybrid vertical levels for the EU nest | 40 |
| 7.1.3. Multi-level fields interpolated to pressure levels | 41 |
| 7.1.4. Single-level fields | 41 |
| 7.1.5. Soil-specific multi-level fields | 45 |
| 7.1.6. Lake-specific single-level fields | 46 |
| 8. Output fields for soil moisture analysis SMA | 47 |
| 9. Extended description of available output fields | 49 |
| 9.1. Cloud products | 49 |
| 9.2. Atmospheric products | 49 |
| 9.3. Near surface products | 49 |
| 9.3.1. General comment on statistically processed fields | 50 |
| 9.4. Surface products | 50 |
| 9.5. Soil products | 51 |
| 9.6. Vertical Integrals | 52 |

| | |
|---|-----------|
| 10. Remarks on statistical processing and horizontal interpolation | 53 |
| 10.1. Statistically processed output fields | 53 |
| 10.1.1. Time-averaged fields | 53 |
| 10.1.2. Accumulated fields | 54 |
| 10.1.3. Extreme value fields | 55 |
| 10.2. Technical Details of the Horizontal Interpolation | 56 |
| 11. ICON data in the SKY data bases of DWD | 57 |
| 11.1. SKY categories for ICON | 57 |
| 11.2. Retrieving ICON data from SKY | 58 |
| Appendix A. ICON standard level heights | 61 |
| A.1. Level heights for zero topography height | 61 |
| A.2. Non-zero topography heights | 61 |
| Bibliography | 67 |
| Glossary | 69 |

1. Introduction

The **ICO**sahedral **N**onhydrostatic model **ICON** is the new global numerical weather prediction model at DWD. It became operational at 2015-01-20, replacing the former operational global model GME. In June 2015 a refined subregion (*nest*) over Europe was activated, which is going to replace the current regional model COSMO-EU during the course of the year 2016. The ICON modelling system as a whole is developed jointly by DWD and the Max-Planck Institute for Meteorology in Hamburg (MPI-M). While ICON is the new working horse for short and medium range global weather forecast at DWD, it embodies the core of a new climate modelling system at MPI-M.

ICON analysis and forecast fields serve as initial and boundary data for a couple of different limited area models: Since 2015-01-20, analysis and forecast fields at 13 km horizontal resolution serve as initial and boundary data for

- the regional model COSMO-EU
- RLMs (**R**elocatable **L**ocal **M**odel) of the German armed forces
- DWD's wave models

Since 2016-07-13 the 6.5 km forecasts of the ICON-EU nest serve as initial and boundary data for

- the regional model COSMO-DE
- the regional ensemble prediction system COSMO-DE-EPS

This document provides some basic information about ICON's horizontal and vertical grid structure, numerical algorithms (see also [Zängl et al. \(2015\)](#)) and physical parameterizations (the latter two are planned but not yet available). Furthermore, it provides an overview about the available ICON analysis and forecast fields stored in the database SKY at DWD. Some examples on how to read these data from the database are given as well.

If you encounter bugs or inconsistencies, or if you have suggestions for improving this document, please contact one of the following colleagues:

Daniel Reinert, FE13
Tel: +49 (69) 8062-2060
Mail: daniel.reinert@dwd.de

Helmut Frank, FE13
Tel: +49 (69) 8062-2742
Mail: helmut.frank@dwd.de


Florian Prill, FE13
Tel: +49 (69) 8062-2727
Mail: florian.prill@dwd.de

2. History of model changes

The forecasting environment, which is composed of the ICON model and the data assimilation system, is subject to continuous improvements and modifications. The most important ones in terms of forecast quality and output products are depicted below. For additional information, the reader is referred to the official change notifications which are available from

http://www.dwd.de/DE/fachnutzer/forschung_lehre/numerische_wettervorhersage/nwv_aenderungen/nwv_aenderungen_node.html

Alternatively you can click on the timeline-date to see the corresponding change notification.

- 
- A vertical timeline with a central line. Blue dots mark most events, while red dots mark the events on 2015-09-02 and 2016-01-20. Each date is followed by a description of the change.
- 2015-01-20** — First operational ICON forecast run at a horizontal resolution of 13 km and 90 vertical levels. Model top at 75 km
 - 2015-02-25** — 4 additional forecast runs 03, 09, 15, 21 UTC up to 30 h lead time. Maximum forecast lead times for 06 and 18 UTC runs extended to 120 h
 - 2015-03-04** — Improved wind gust diagnostic for mountainous regions
 - 2015-07-07** — Time interval over which max/min temperatures TMAX_2M, TMIN_2M are collected changed to 6 h (formerly 3 h). Time interval over which maximum wind gusts VMAX_10M are collected changed to 1 h (formerly 3 h).
 - 2015-07-21** — Launch of the ICON-EU nest with a horizontal resolution of 6.5 km and 50 vertical levels. Model top at 50 km.
 - 2015-09-02** — Assimilation of selected microwave satellite radiance channels over land (AMSU-A and ATMS), which have so far been assimilated only over the oceans.
 - 2015-12-01** — Surface tile approach for land, sea-ice and lake points, including snow-tiles. Each grid point can have up to 5 tiles consisting of 3 land tiles (dominant land-use types), a lake tile or a sea-water plus sea-ice tile. Land tiles may have additional snow tiles.
 - 2016-01-20** — Launch of the ensemble data assimilation system (LETKF, Localized Ensemble Transform Kalman Filter), providing a 40 member analysis ensemble at R2B6N7. For deterministic forecasts the 3D-Var assimilation system is replaced by En-Var (Ensemble Variational analysis system) which makes use of the ensemble-based model error covariances.

- 2016-04-13** —● Improved version of the ICON model which
- accounts for oceanic salt content in the saturation vapor pressure computation.
 - contains modifications to the detrainment tendencies from the convection parameterization in order to reduce spurious drizzle.
 - makes use of the aerosol climatology for the computation of cloud droplet number concentrations in the radiation parameterization.
- 2016-04-20** —● The pressure levels for regular grid output have been revised. Newly available levels: 650, 550, 450, 350, 275, 225, 175, 125 hPa. Deprecated levels: 725, 20, 7, 3, 0.3 hPa.
- 2016-09-28** —● New version of the ICON model in which
- the convection parameterization has been improved with respect to mixed-phase cloud processes
 - the process of rain water evaporation below cloud base has been updated.
-

3. Grid geometry

3.1. Horizontal grid

The horizontal ICON grid consists of a set of spherical triangles that seamlessly span the entire sphere. The grid is constructed from an icosahedron (see Figure 3.1a) which is projected onto a sphere. The spherical icosahedron (Figure 3.1b) consists of 20 equilateral spherical triangles. The edges of each triangle are bisected into equal halves or more generally into n equal sections. Connecting the new edge points by great circle arcs yields 4 or more generally n^2 spherical triangles within the original triangle (Figure 3.2a, 3.2b).



Figure 3.1.: Icosahedron before (a) and after (b) projection onto a sphere

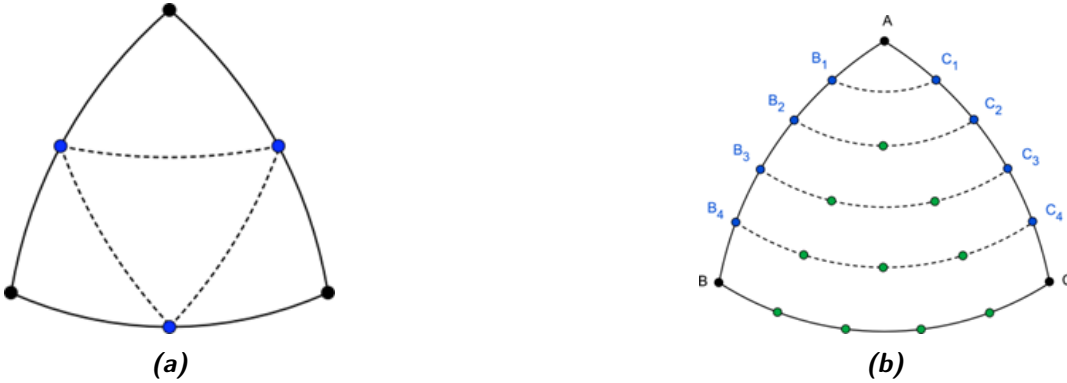


Figure 3.2.: (a) Bisection of the original triangle edges (b) More general division into n equal sections

ICON grids are constructed by an initial root division into n sections (\mathbf{R}_n) followed by k bisection steps (\mathbf{B}_k), resulting in a $\mathbf{R}_n\mathbf{B}_k$ grid. Figures 3.3a and 3.3b show $\mathbf{R}_2\mathbf{B}_0$ and $\mathbf{R}_2\mathbf{B}_2$ ICON grids. Such grids avoid polar singularities of latitude-longitude grids (Figure 3.3c) and allow a high uniformity in resolution over the whole sphere.

Throughout this document, the grid is referred to as the “ $\mathbf{R}_n\mathbf{B}_k$ grid” or “ $\mathbf{R}_n\mathbf{B}_k$ resolution”. For a



Figure 3.3.: (a) R2B00 grid. (b) R2B02 grid. (c) traditional regular latitude-longitude grid with polar singularities

given resolution \mathbf{RnBk} , the total number of cells, edges, and vertices can be computed from

$$\begin{aligned} n_c &= 20 n^2 4^k \\ n_e &= 30 n^2 4^k \\ n_v &= 10 n^2 4^k + 2 \end{aligned}$$

The average cell area $\overline{\Delta A}$ can be computed from

$$\overline{\Delta A} = \frac{4\pi r_e^2}{n_c},$$

with the earth radius r_e , and n_c the total number of cells. ICON uses an earth radius of

$$r_e = 6.371229 \cdot 10^6 \text{ m.}$$

Based on $\overline{\Delta A}$ one can derive an estimate of the average grid resolution $\overline{\Delta x}$:

$$\overline{\Delta x} = \sqrt{\overline{\Delta A}} = \sqrt{\frac{\pi}{5} \frac{r_e}{n 2^k}}$$

Visually speaking, $\overline{\Delta x}$ is the edge length of a square which has the same area as our triangular cell.

In Table 3.1, some characteristics of frequently used ICON grids are given. The table contains information about the total number of triangles (n_c), the average resolution $\overline{\Delta x}$, and the maximum/minimum cell area. The latter may be interpreted as the area for which the prognosed meteorological quantities (like temperature, pressure, ...) are representative. Some additional information about ICON's horizontal grid can be found in [Wan et al. \(2013\)](#).

Table 3.1.: Characteristics of frequently used ICON grids. ΔA_{\max} and ΔA_{\min} refer to the maximum and minimum area of the grid cells, respectively.

| Grid | number of cells (n_c) | avg. resolution [km] | ΔA_{\max} [km ²] | ΔA_{\min} [km ²] |
|-------|---------------------------|----------------------|--------------------------------------|--------------------------------------|
| R2B04 | 20480 | 157.8 | 25974.2 | 18777.3 |
| R2B05 | 81920 | 78.9 | 6480.8 | 4507.5 |
| R2B06 | 327680 | 39.5 | 1618.4 | 1089.6 |
| R2B07 | 1310720 | 19.7 | 404.4 | 265.1 |
| R3B07 | 2949120 | 13.2 | 179.7 | 116.3 |

The first operational version of ICON is based on the R3B07 grid, thus, having a horizontal resolution of about 13 km!

3.2. Vertical grid

The vertical grid consists of a set of vertical layers with height-based vertical coordinates. Each of these layers carries the horizontal 2D grid structure, thus forming the 3D structure of the grid. The ICON grid employs a Lorenz-type staggering with the vertical velocity defined at the boundaries of layers (half levels) and the other prognostic variables in the center of the layer (full levels).

To improve simulations of flow past complex topography, the ICON model employs a smooth level vertical (SLEVE) coordinate (Leuenberger et al., 2010). It allows for a faster transition to smooth levels in the upper troposphere and lower stratosphere, as compared to the classical height-based Gal-Chen coordinate. In the operational setup, the transition from terrain following levels in the lower atmosphere to constant height levels is completed at $z = 16$ km. Model levels above are flat. The required smooth large-scale contribution of the model topography is generated by digital filtering with a ∇^2 -diffusion operator. Figure 3.4 shows the (half) levels of the operational ICON setup with 90 vertical levels. The table to the right shows the height above ground of selected half levels (for zero height topography) and the corresponding pressure, assuming the US standard atmosphere. Standard heights for all 91 half levels are given in Table A.1.

Please note that for grid cells with non-zero topography these values only represent rough estimates of the true level height. Actual heights and layer thicknesses may vary considerably from location to location, due to grid level stretching/compression over non-zero topography.

3.3. Refined subregion over Europe (“local nest”)

ICON has the capability for running global simulations with refined domains (so called *nests*). The triangular mesh of the refined area is generated by bisection of triangles in the global “parent” grid, see Fig. 3.5. In the vertical the global grid extends into the mesosphere (which greatly facilitates the assimilation of satellite data) whereas the nested domains extend only into the lower stratosphere in order to save computing time. For the same orography the heights of levels 1–60 of the Europe nest are the same as those of levels 31–90 of the global grid. In practice, however, near surface level heights of nests and the global domain differ due to the fact that the underlying orography differs, with deeper slopes and higher summits in the high resolution nests.

For each nesting level, the time step is automatically divided by a factor of two. Note that the grid nests are computed in a concurrent fashion:

- Points that are covered by the refined subdomain additionally contain data for the global grid state.
- The data points on the triangular grid are the cell circumcenters. Therefore the global grid data points are closely located to nest data sites, but they *do not coincide* exactly (see Fig. 3.5).

ICON’s refined subregion over Europe is comparable to the COSMO-EU region of DWD’s COSMO model. Key figures like edge coordinates and mesh size of the COSMO-EU region and the ICON-EU nest are given in Table 3.2. The geographical location of the nest is visualized in Fig. 3.6a and Fig. 3.6b.

Model simulations including the nesting region over Europe are running regularly, starting from

2015-07-21, 06 UTC (roma).

Main forecasts starting at 00, 06, 12, 18 UTC reach out to 120 h, while additional short-range forecasts starting at 03, 09, 15, 21 UTC provide data until +30 h.

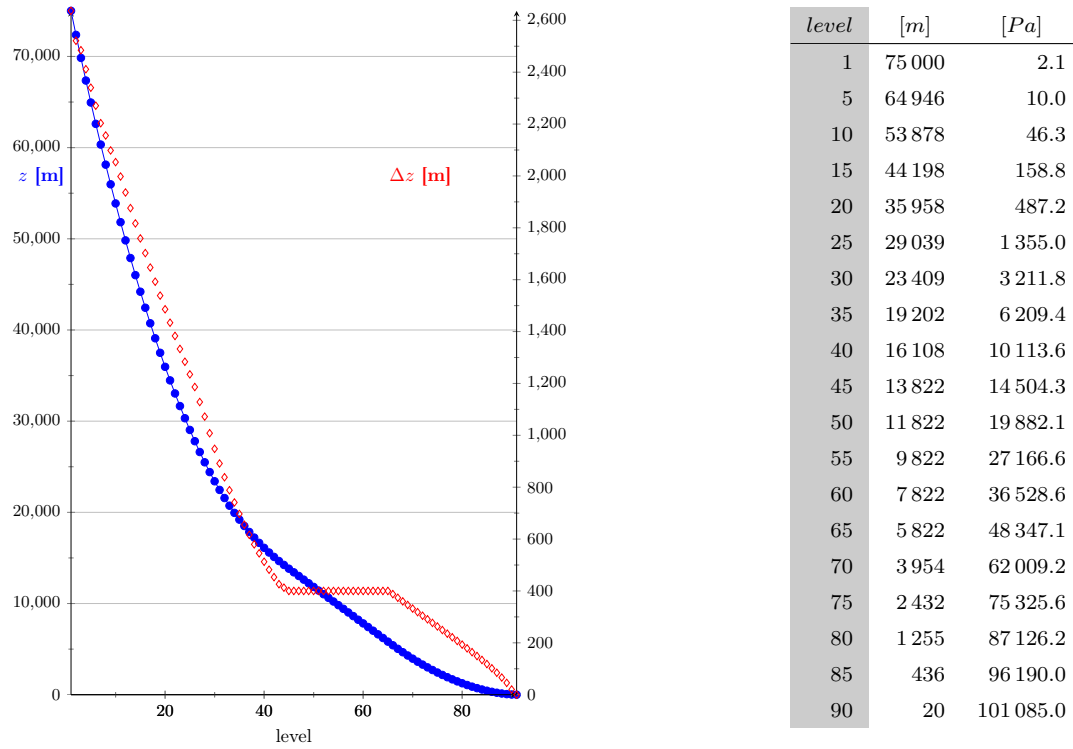


Figure 3.4.: Vertical half levels (blue) and layer thickness (red) of the ICON operational setup. The table of selected pressure values (for zero height) is based on the 1976 US standard atmosphere.

Simulation on the global grid and the regional (Europe) domain are tightly coupled (*two-way nesting*): Boundary data for the nest area is updated every time step (120 s). Feedback of atmospheric prognostic variables (except precipitation) is computed via relaxation on a 3 h time scale.



Figure 3.5.: ICON grid refinement (zoom view). Blue and red dots indicate the cell circumcenters for the global (“parent”) and the refined (“child”) domain, respectively.

Table 3.2.: Key figures of the ICON-EU nest and the COSMO-EU region.

| | ICON-EU nest | COSMO-EU |
|--------------------|--|---|
| geogr. coordinates | 23.5° W – 62.5° E 29.5° N – 70.5° N | $\lambda_N = 170^\circ$ W, $\phi_N = 40^\circ$ N, 18.0° W – 23.5° E 20.0° S – 21.0° N |
| mesh size | ≈ 6.5 km (R3B08) 659156 triangles | 0.0625° (≈ 7 km) $665 \times 657 = 436905$ grid points |
| vertical levels | 60 levels | 40 levels |
| upper boundary | 22.5 km | 22.5 km |

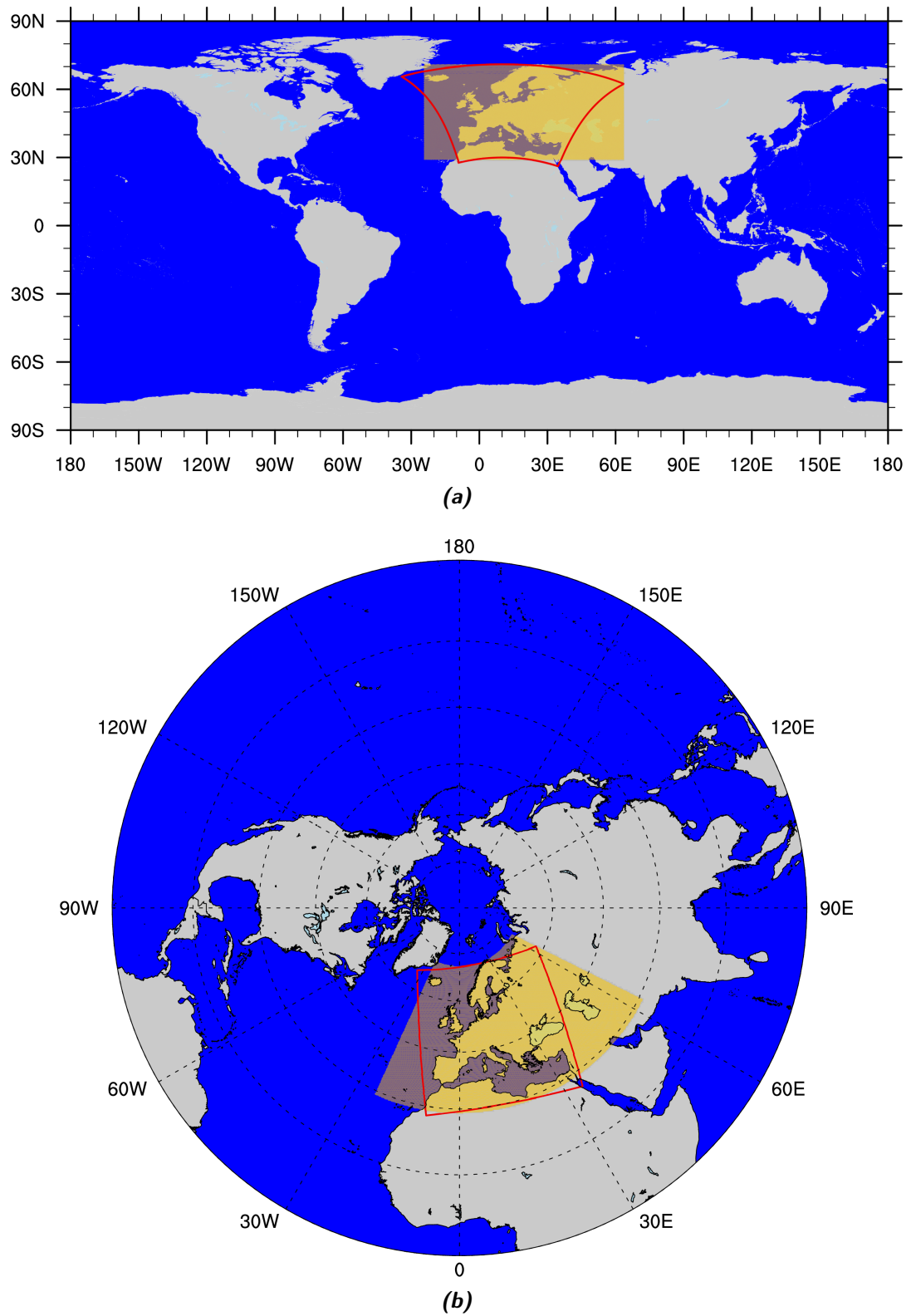


Figure 3.6.: 3.6a: Horizontal extent of the ICON-EU nest (orange shaded area) in a cylindrical equidistant projection. For comparison, the outline of the COSMO-EU region is shown in red. 3.6b: Same as 3.6a but in a polar stereographic projection.

4. Mandatory input fields

Several input files are needed to perform runs of the ICON model. These can be divided into three classes: Grid files, external parameters, and initialization (analysis) files. The latter will be described in Chapter 5.

4.1. Grid Files

In order to run ICON, it is necessary to load the horizontal grid information as an input parameter. This information is stored within so-called grid files. For an ICON run, at least one global grid file is required. For model runs with nested grids, additional files of the nested domains are necessary. Optionally, a reduced radiation grid for the global domain may be used.

The unstructured triangular ICON grid resulting from the grid generation process is represented in NetCDF format. The most important data entries are

- **cell** (INTEGER dimension)
number of (triangular) cells
- **vertex** (INTEGER dimension)
number of triangle vertices
- **edge** (INTEGER dimension)
number of triangle edges
- **clon, clat** (double array, dimension: #triangles, given in radians)
longitude/latitude of the triangle circumcenters
- **vlon, vlat** (double array, dimension: #triangle vertices, given in radians)
longitude/latitude of the triangle vertices
- **elon, elat** (double array, dimension: #triangle edges, given in radians)
longitude/latitude of the edge midpoints
- **cell_area** (double array, dimension: #triangles)
triangle areas
- **vertex_of_cell** (INTEGER array, dimensions: [3, #triangles])
The indices `vertex_of_cell(:,i)` denote the triangle vertices that belong to the triangle `i`.
- **edge_of_cell** (INTEGER array, dimensions: [2, #triangles])
The indices `edge_of_cell(:,i)` denote the triangle edges that belong to the triangle `i`.

4.2. External parameters

External parameters are used to describe the properties of the earth's surface. These data include the orography and the land-sea-mask. Also, several parameters are needed to specify the dominant land use of a grid box like the soiltype or the plant cover fraction.

The ExtPar software (ExtPar – External parameter for Numerical Weather Prediction and Climate Application) is able to generate external parameters for the ICON model. The generation is based on a set of raw-datafields which are listed in Table 4.1. For a more detailed overview of ExtPar, the reader is referred to the *User and Implementation Guide* of Extpar.

Table 4.1.: Raw datasets from which the ICON external parameter fields are derived.

| Dataset | Source | Resolution |
|-------------------------------------|---|------------|
| GLOBE orography | NOAA/NGDC | 30" |
| GlobCover 2009 | ESA | 10" |
| GLCC land use | USGS | 30" |
| HWSD Harmonized World Soil Database | FAO/IIASA/ISRIC/ISSCAS/JRC | 30" |
| NDVI Climatotology, SeaWiFS | NASA/GSFC | 2.5' |
| CRU near surface climatology | CRU University of East Anglia | 0.5° |
| GACP Aerosol Optical thickness | NASA/GISS (Global Aerosol Climatology Project) | 4x5° |
| GLDB Global lake database | DWD/RSHU/MeteoFrance | 30" |
| MODIS albedo | NASA | 5' |

GlobCover 2009 is a land cover database covering the whole globe, except for Antarctica. Therefore, we make use of *GlobCover 2009* for $90^\circ > \phi > -56^\circ$ (with ϕ denoting latitude) and switch to the coarser, however globally available dataset *GLCC* for $-56^\circ \geq \psi > -90^\circ$.

The products generated by the ExtPar software package are listed in Table 4.2 together with the underlying raw dataset. Note that these are mandatory input fields for assimilation- and forecast runs.

Table 4.2.: External parameter fields for ICON, produced by the ExtPar software package (in alphabetical order)

| ShortName | Description | Raw dataset |
|------------|--|----------------|
| AER_SS12 | Sea salt aerosol climatology (monthly fields) | GACP |
| AER_DUST12 | Total soil dust aerosol climatology (monthly fields) | GACP |
| AER_ORG12 | Organic aerosol climatology (monthly fields) | GACP |
| AER_SO412 | Total sulfate aerosol climatology (monthly fields) | GACP |
| AER_BC12 | Black carbon aerosol climatology (monthly fields) | GACP |
| ALB_DIF12 | Shortwave (0.3 – 5.0 μm) albedo for diffuse radiation (monthly fields) | MODIS |
| ALB_UV12 | UV-visible (0.3 – 0.7 μm) albedo for diffuse radiation (monthly fields) | MODIS |
| ALB_NI12 | Near infrared (0.7 – 5.0 μm) albedo for diffuse radiation (monthly fields) | MODIS |
| DEPTH_LK | Lake depth | GLDB |
| EMIS_RAD | Surface longwave (thermal) emissivity | GlobCover 2009 |
| FOR_D (*) | Fraction of deciduous forest | GlobCover 2009 |
| FOR_E (*) | Fraction of evergreen forest | GlobCover 2009 |

Continued on next page

Table 4.2.: *continued*

| | | |
|--------------|--|----------------|
| FR_LAKE | Lake fraction (fresh water) | GLDB |
| FR_LAND | Land fraction (excluding lake fraction but including glacier fraction) | GlobCover2009 |
| FR_LUC | Landuse class fraction | |
| HSURF | Orography height at cell centres | GLOBE |
| LAI_MX (*) | Leaf area index in the vegetation phase | GlobCover 2009 |
| NDVI_MAX | Normalized differential vegetation index | SeaWiFS |
| NDVI_MRAT | proportion of monthly mean NDVI to yearly maximum (monthly fields) | SeaWiFS |
| PLCOV_MX (*) | Plant covering degree in the vegetation phase | GlobCover 2009 |
| ROOTDP (*) | Root depth | GlobCover 2009 |
| RSMIN (*) | Minimum stomatal resistance | GlobCover 2009 |
| SOILTYP | Soil type | HWSD |
| SSO_STDH | Standard deviation of sub-grid scale orographic height | GLOBE |
| SSO_THETA | Principal axis-angle of sub-grid scale orography | GLOBE |
| SSO_GAMMA | Horizontal anisotropy of sub-grid scale orography | GLOBE |
| SSO_SIGMA | Average slope of sub-grid scale orography | GLOBE |
| T_2M_CL | Climatological 2m temperature (serves as lower boundary condition for soil model) | CRU |
| Z0 (*) | Surface roughness length (over land), containing a contribution from subgrid-scale orography | GlobCover 2009 |

Note that fields marked with (*) are not required in operational model runs. I.e. the surface roughness Z0 is only needed, if the additional contribution from sub-grid scale orography is taken into account (i.e. for `itype_z0=1`). In operational runs, land-cover class specific roughness lengths are taken from a GlobCover-based lookup table. `FOR_D`, `FOR_E`, `LAI_MX`, `PLCOV_MX`, `RSMIN`, and `ROOTDP` became obsolete with the activation of the surface tile approach (2015-03-04). The latter 4 fields are replaced by land-cover class specific values taken from lookup tables.

Remarks on post-processing

Some of the external parameter fields produced by ExtPar are modified by ICON. The following fields are affected:

| | | | | |
|----------|-------|---------|---------|----|
| DEPTH_LK | HSURF | FR_LAND | FR_LAKE | Z0 |
|----------|-------|---------|---------|----|

Thus, for consistency, the modified fields should be used for post-processing tasks rather than the original external parameter fields. See Section 6.3.1 for more details.

5. Analysis fields

Numerical weather prediction (NWP) is an initial value problem. The ability to make a skillful forecast relies heavily on an accurate estimate of the present atmospheric state, known as the analysis. In general, an analysis is generated by optimally combining all available observations with a short-range model forecast, known as *first guess* (FG) or *background*. Currently an atmospheric analysis is created every 3 h. The 3-hourly first guess output provided by ICON comprises the following fields:

Table 5.1.: Available 3 h first guess output fields from the forecast database
CAT_NAME=\$model_ass_fc_\$suite

| Type | GRIB shortName |
|-----------------------|---|
| Atmosphere | VN, U, V, W, DEN, THETA_V, T, QV, QC, QI, QR, QS, TKE, P |
| Surface (general) | T_G, T_SO(0), QV_S, T_2M, TD_2M, U_10M, V_10M, PS, Z0 |
| Land specific | W_SNOW, T_SNOW, RHO_SNOW, H_SNOW, FRESHSNW, W_I, T_SO(1:nlev_soil), W_SO, W_SO_ICE |
| Lake/sea ice specific | T_MNW_LK, T_WML_LK, H_ML_LK, T_BOT_LK, C_T_LK, T_B1_LK, H_B1_LK, T_ICE, H_ICE, FR_ICE |
| Time invariant | FR_LAND, HHL, CLON, CLAT, ELON, ELAT, VLON, VLAT |

Atmospheric analysis fields are computed every 3 hours (00, 03, 06, ... 21 UTC) by the 3DVar data assimilation system, which has recently been upgraded to an En-Var system (see Section 5.1). Sea surface temperature T_SO(0) and sea ice cover FR_ICE are provided once per day (00 UTC) by the SST-Analysis. A snow analysis is conducted every 3 hours, providing updated information on the snow height H_SNOW and snow age FRESHSNW. In addition a soil moisture analysis (SMA) is conducted once per day (00 UTC). It basically modifies the soil moisture content W_SO, in order to improve the 2 m temperature forecast.

For the 3-hourly assimilation cycle and forecast runs, ICON must be provided with 2 input files: One containing the First Guess (FG) and the other containing analysis (AN) fields, only. Variables for which no analysis is available are always read from the first guess file (e.g. TKE). Other variables may be read either from the first guess or the analysis file, depending on the starting time. E.g. for T_SO(0) the first guess is read at 03, 06, 09, 12, 15, 18, 21 UTC, however, the analysis is read at 00 UTC when a new SST analysis is available. In Table 5.2 the available and employed first guess and analysis fields are listed as a function of starting time.

Table 5.2.: The leftmost column shows variables that are mandatory for the assimilation cycle and forecast runs. Column 2 indicates, whether or not an analysis is performed for these variables. Columns 3 to 10 show the origin of these variables (analysis or first guess), depending on the starting time.

| ShortName | Analysis | 00 | 03 | 06 | 09 | 12 | 15 | 18 | 21 |
|-----------------------|----------|----|----|----|----|----|----|----|----|
| Atmosphere | | | | | | | | | |
| VN | – | FG | FG | FG | FG | FG | FG | FG | FG |
| THETA_V | – | FG | FG | FG | FG | FG | FG | FG | FG |
| DEN | – | FG | FG | FG | FG | FG | FG | FG | FG |
| W | – | FG | FG | FG | FG | FG | FG | FG | FG |
| TKE | – | FG | FG | FG | FG | FG | FG | FG | FG |
| QC, QI, QR, QS | – | FG | FG | FG | FG | FG | FG | FG | FG |
| QV | 3DVar | AN | AN | AN | AN | AN | AN | AN | AN |
| T | 3DVar | AN | AN | AN | AN | AN | AN | AN | AN |
| P | 3DVar | AN | AN | AN | AN | AN | AN | AN | AN |
| U, V | 3DVar | AN | AN | AN | AN | AN | AN | AN | AN |
| Surface | | | | | | | | | |
| Z0 | – | FG | FG | FG | FG | FG | FG | FG | FG |
| T_G | – | FG | FG | FG | FG | FG | FG | FG | FG |
| QV_S | – | FG | FG | FG | FG | FG | FG | FG | FG |
| T_SO(0) (SST only) | Ana_SST | AN | FG | FG | FG | FG | FG | FG | FG |
| T_SO(0:nlevsoil) | – | FG | FG | FG | FG | FG | FG | FG | FG |
| W_SO_ICE | – | FG | FG | FG | FG | FG | FG | FG | FG |
| W_SO | SMA | AN | FG | FG | FG | FG | FG | FG | FG |
| W_I | – | FG | FG | FG | FG | FG | FG | FG | FG |
| W_SNOW ¹ | Ana_SNOW | AN | AN | AN | AN | AN | AN | AN | AN |
| T_SNOW | – | FG | FG | FG | FG | FG | FG | FG | FG |
| RHO_SNOW ¹ | Ana_SNOW | AN | AN | AN | AN | AN | AN | AN | AN |
| H_SNOW | Ana_SNOW | AN | AN | AN | AN | AN | AN | AN | AN |
| FRESHSNW | Ana_SNOW | AN | AN | AN | AN | AN | AN | AN | AN |
| SNOWC | – | FG | FG | FG | FG | FG | FG | FG | FG |
| Sea ice/Lake | | | | | | | | | |
| T_ICE | – | FG | FG | FG | FG | FG | FG | FG | FG |
| H_ICE | – | FG | FG | FG | FG | FG | FG | FG | FG |
| FR_ICE | Ana_SST | AN | FG | FG | FG | FG | FG | FG | FG |

Continued on next page

Table 5.2.: The leftmost column shows variables that are mandatory for the assimilation cycle and forecast runs. Column 2 indicates, whether or not an analysis is performed for these variables. Columns 3 to 10 show the origin of these variables (analysis or first guess), depending on the starting time.

| ShortName | Analysis | 00 | 03 | 06 | 09 | 12 | 15 | 18 | 21 |
|-----------|----------|----|----|----|----|----|----|----|----|
| T_MNW_LK | – | FG | FG | FG | FG | FG | FG | FG | FG |
| T_WML_LK | – | FG | FG | FG | FG | FG | FG | FG | FG |
| H_ML_LK | – | FG | FG | FG | FG | FG | FG | FG | FG |
| T_BOT_LK | – | FG | FG | FG | FG | FG | FG | FG | FG |
| C_T_LK | – | FG | FG | FG | FG | FG | FG | FG | FG |
| T_B1_LK | – | FG | FG | FG | FG | FG | FG | FG | FG |
| H_B1_LK | – | FG | FG | FG | FG | FG | FG | FG | FG |

5.1. Ensemble Data Assimilation

Until 2016-01-20 the analyses were derived by a 3-hourly cycled 3-dimensional data assimilation system (3D-Var).

From 2016-01-20 on the analysis system consists of the 3-hourly cycled Ensemble Variational Data assimilation system (En-Var) providing initial fields for the deterministic ICON forecasts at 13 km resolution, based on the 3-hour short range forecast (first guess) and the observations at the actual analysis time. In the En-Var a part of the background error covariance matrix is derived from the statistics of a 3-hour short range ensemble forecast at lower resolution (currently 40 members at 40 km R2B06 resolution with a 20 km nest over Europe). The En-Var deterministic analysis system is complemented by an Ensemble Data Assimilation system (EDA), in the specific implementation of a Localized Ensemble Transform Kalman Filter (LETKF). The EDA provides the initial fields for the 3-hourly cycled ICON short range ensemble forecasts.

Both the deterministic and the ensemble data assimilation provide atmospheric analyses and analysis increments as described in Table 5.2 and Section 5.2. However, The Ensemble Data assimilation currently does not run separate analyses for sea surface temperature, snow, and soil moisture. Instead these fields are derived from the deterministic forecast and provided 3-hourly by the EDA in the following way:

Sea Surface Temperature The sea surface temperature at ensemble resolution is interpolated (taking the nearest neighbor) from the deterministic sea surface temperature. Ice fraction, ice height, and ice temperature are taken from the deterministic first guess as well. As a SST analysis is run once a day in the deterministic forecast system this mechanism ensures that the ensemble sea surface temperature stays close to the observed one.

In addition the interpolated sea surface temperature is perturbed individually for each ensemble member with prescribed spatial and temporal correlation length scales to account for the uncertainties in the SST analysis.

¹Note that `RHO_SNOW` is read from the analysis, however it does not contain any new/independent information compared to the model first guess, except for an initialization of newly generated snow points and a limitation over glacier points. `W_SNOW` is read from the analysis, too, however it is re-diagnosed within the ICON-code based on the analyzed snow height `H_SNOW` and the former mentioned snow density `RHO_SNOW`.

Soil Moisture

The ensemble mean of soil moisture is adjusted to its value in the deterministic run. This procedure ensures that the mean ensemble soil moisture stays close to the analyzed one, as a soil moisture analysis is run once a day in the deterministic forecast system. By adjusting only the ensemble mean the ensemble spread is preserved.

Snow

For each ensemble member the mean ensemble snow cover is adjusted to its deterministic value.

The data assimilation system also provides a couple of fields, which are not modified with respect to their guess values, so that a full set of nominal analysis fields is available.

Table 5.3.: Fields provided by the ensemble analysis system. The column **Increment** indicates if an analysis increment is provided. **Analysis** indicates if the field is analysed by the LETKF (letkf), taken from the first guess (fg), interpolated (det) from, or (mean) adjusted to the respective deterministic quantity, or additionally perturbed (per).

| ShortName | Type | Increment | Analysis | |
|-----------|-------------|-----------|----------|----------------------------|
| T | Atmosphere | yes | letkf | Temperature |
| U | " | yes | letkf | U-Component of Wind |
| V | " | yes | letkf | V-Component of Wind |
| QV | " | yes | letkf | Specific Humidity |
| P | " | yes | letkf | Pressure |
| QC | " | | letkf | Cloud Mixing Ratio |
| QI | " | | letkf | Cloud Ice Mixing Ratio |
| QR | " | | fg | Rain Mixing Ratio |
| QS | " | | fg | Snow Mixing Ratio |
| H_SNOW | Snow | yes | mean | Snow Depth |
| FRESHSNW | " | yes | mean | Fresh snow factor |
| QV_S | Surface | | fg | Surface Specific Humidity |
| W_I | " | | fg | Plant Canopy Surface Water |
| Z0 | " | | fg | Surface Roughness length |
| T_SO(0) | Sea surface | | det+per | Sea Surface Temperature |
| H_ICE | " | | det | Sea Ice Thickness |
| FR_ICE | " | | det | Sea Ice Cover |
| W_SO | Soil | yes | mean | Soil moisture |
| W_SO_ICE | " | | fg | Soil ice content |
| T_SO | " | | fg | Soil temperature |

5.2. Incremental analysis update

Analysis fields provided by the data assimilation system are usually not perfectly balanced, leading to e.g. the generation of spurious gravity waves. Thus, atmospheric models generally require some initialization procedure in order to minimize spin-up effects and to prevent the accumulation of noise. In ICON, a method known as **Incremental Analysis Update (IAU)** (Bloom et al., 1996, Polavarapu et al., 2004) is applied. The basic idea is quite simple: Rather than adding the analysis increments $\Delta \mathbf{x}^A = \mathbf{x}^A - \mathbf{x}^{FG}$ (i.e. the difference between the analysis \mathbf{x}^A and the model first guess \mathbf{x}^{FG}) in one go, they are incorporated into the model in small drips over many timesteps (see Figure 5.1).



Figure 5.1.: Incremental Analysis Update. Analysis increments are added to the background state (FG) in small drips over some time interval rather than in one go. Currently, increments for U, V, P, T, QV are treated in this way.

Mathematically speaking, during forward integration the model is forced with appropriately weighted analysis increments:

$$\frac{d\mathbf{x}}{dt} = A\mathbf{x} + g(t)\Delta\mathbf{x}^A \quad , \text{ with } \int g(t) dt = 1 \quad (5.1)$$

\mathbf{x} is the discrete model state, A is a matrix representing the (non)-linear dynamics of the system and $g(t)$ is a weighting function, which is non-zero over some time-interval Δt .

This drip by drip incorporation acts as a low pass filter in frequency domain on the analysis increments such that small scale unbalanced modes are effectively filtered (see Bloom et al. (1996)). The filter characteristic depends on the weighting function $g(t)$. It should be noted that IAU only filters the increments and not the background state, such that regions where analysis increments are zero remain unaffected. This method is currently applied to the prognostic atmospheric fields π , ρ , v_n , q_v , based on analysis increments provided for u , v , p , t and q_v . π denotes the Exner pressure.

The method sounds incredibly simple, however there are a few technical aspects to be taken care of when implementing this into an operational system: Figure 5.2 shows how the IAU-method is implemented in ICON for a 3 h assimilation run starting at midnight. Analysis increments are applied over a 3 h time window, centered at the actual model start time. As indicated by the blue line, constant weights are used:

$$g(t) = \frac{\Delta t}{T} \quad , \text{ for } -T/2 < t < T/2 \quad (5.2)$$

T is the window width and Δt is the fast physics time step. The key point in terms of technical implementation is that the model must be started 90 minutes prior to the actual starting time of the assimilation run. The model is started from the 22:30 UTC first guess. The analysis increments for U, V, P, T, QV , whose validity time is 00:00 UTC are added over 3 hours until at 1:30 the free forecast starts. Then, two first guess data sets are written into the database. One at 1:30 UTC, which will be used for starting the next 3 h assimilation run, and a second one at 3:00 UTC, which serves as input for the assimilation system itself. Thus in general, using the IAU method requires some care in terms of reading and writing the right fields at the right times.

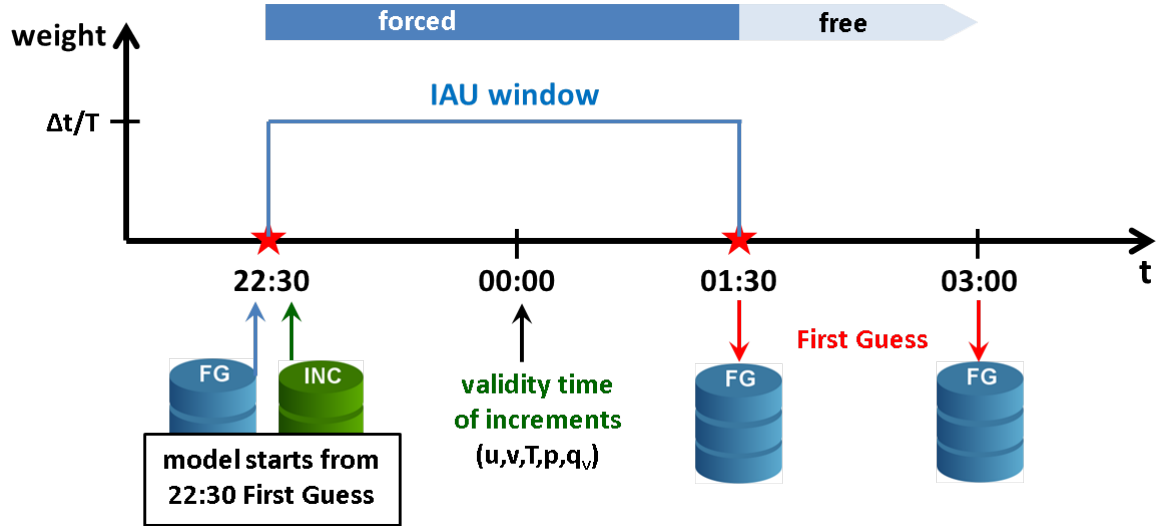


Figure 5.2.: Time line for an ICON assimilation run starting at 00:00 UTC.

This method is not restricted to atmospheric fields, but also applied to assimilated soil and surface fields, specifically soil moisture W_{SO} , and snow quantities H_{SNOW} and $FRESHSNW$.

6. Global output fields: Forecast runs

ICON output fields are exclusively available in GRIB2 format (**GR**Idded **B**inary Edition **2**), with the exception of meteogram data (NetCDF). GRIB is a bit-oriented data storage format which was developed by [World Meteorological Organization \(WMO\)](#) to facilitate the exchange of large volumes of gridded data between weather prediction centres. For decoding and encoding GRIB2 messages, the DWD in general and ICON in particular makes use of the ECMWF GRIB API. The current operational version at DWD is 1.13.1.

In GRIB2, a product (i.e. a variable/field) is identified by a set of three parameters

- *Discipline* (see GRIB2 code table 0.0)
- *ParameterCategory* (see GRIB2 code table 4.1)
- *ParameterNumber* (see GRIB2 code table 4.2),

augmented by a large number of additional metadata in order to uniquely describe the nature of the data. Noteworthy examples of additional metadata are

- *typeOfFirstFixedSurface* and *typeOfSecondFixedSurface* (see GRIB2 code table 4.5)
- *typeOfStatisticalProcessing*, former known as *stepType* (instant, accum, avg, max, min, diff, rms, sd, cov, ...), describing the statistical process used to calculate the field

just to name a few.

A documentation of the official WMO GRIB2 code tables can be found here:

http://www.wmo.int/pages/prog/www/WMOCodes/WMO306_vI2/LatestVERSION/WMO306_vI2_GRIB2_CodeFlag_en.pdf

In the following tables *typeOfFirstFixedSurface* and *typeOfSecondFixedSurface* will be abbreviated by *Lev-Typ 1/2*.

6.1. Deprecated output fields

With the launch of ICON, the following former GME output fields are no longer available:

- **BAS_CON** [-]: Level index of convective cloud base. Instead, **HBAS_CON** [m] should be used.
- **TOP_CON** [-]: Level index of convective cloud top. Instead, **HTOP_CON** [m] should be used.
- **W_G1**, **W_G2** [mm H₂O]: Soil water content in upper layer (0 to 10 cm) and middle layer (10 to 100 cm), respectively. If needed, these fields can be derived from **W_SO**.
- **FIS** [m² s⁻¹]: Surface Geopotential. Instead, **HSURF** [m] should be used (see Section 6.2).
- **O3** [kg/kg], **TO3** [Dobson]: Ozone mixing ratio and corresponding total ozone concentration. No longer available; no substitution

6.2. New output fields

Table 6.1 contains a list of new output fields that became available with the launch of ICON (compared to GME). A more thorough description of these fields is provided in Section 6.3.

Table 6.1.: Newly available output fields

| ShortName | Unit | Description |
|-------------------|----------------------------|--|
| Atmosphere | | |
| DEN | kg m^{-3} | Density of moist air (3D field) |
| TKE | $\text{m}^2 \text{s}^{-2}$ | Turbulent kinetic energy (3D field) |
| DTKE_CON | $\text{m}^2 \text{s}^{-3}$ | Buoyancy-production of TKE due to sub grid scale convection (3D field) |
| DTKE_HSH | $\text{m}^2 \text{s}^{-3}$ | Production of TKE due to horizontal shear (3D field) |
| W | m s^{-1} | Vertical velocity in height coordinates $w = \frac{dz}{dt}$ (3D field) |
| P | Pa | Pressure (3D field) |
| Surface | | |
| CAPE_CON | J kg^{-1} | Convective available potential energy (2D field) |
| QV_2M | kg kg^{-1} | Specific humidity at 2m above ground (2D field) |
| RELHUM_2M | % | Relative humidity at 2m above ground (2D field) |
| SOBS_RAD | W m^{-2} | Net short-wave radiation flux at surface (instantaneous) |
| THBS_RAD | W m^{-2} | Net long-wave radiation flux at surface (instantaneous) |
| Lake | | |
| C_T_LK | 1 | Shape factor with respect to the temperature profile in the thermocline (2D field) |
| H_ML_LK | m | Mixed-layer depth (2D field) |
| T_BOT_LK | K | Temperature at the water-bottom sediment interface (2D field) |
| T_MNW_LK | K | Mean temperature of the water column (2D field) |
| T_WML_LK | K | Mixed-layer temperature (2D field) |
| Geometry | | |
| HSURF | m | Geometric Height of the earths surface above sea level (2D field) |
| HHL | m | Geometric Height of model half levels above sea level (3D field) |
| CLON,CLAT | deg | Geographical longitude/latitude of native grid triangle cell center |
| ELON,ELAT | deg | Geographical longitude/latitude of native grid triangle edge mid-point |

6.3. Available output fields

ICON forecasts are performed multiple times a day with varying forecast periods. An overview of the forecast runs, including its forecast period and output intervals is provided in Figure 6.1.

Main forecasts are performed 4 times a day at 0, 6, 12, 18 UTC, covering a forecast time span of 180 h

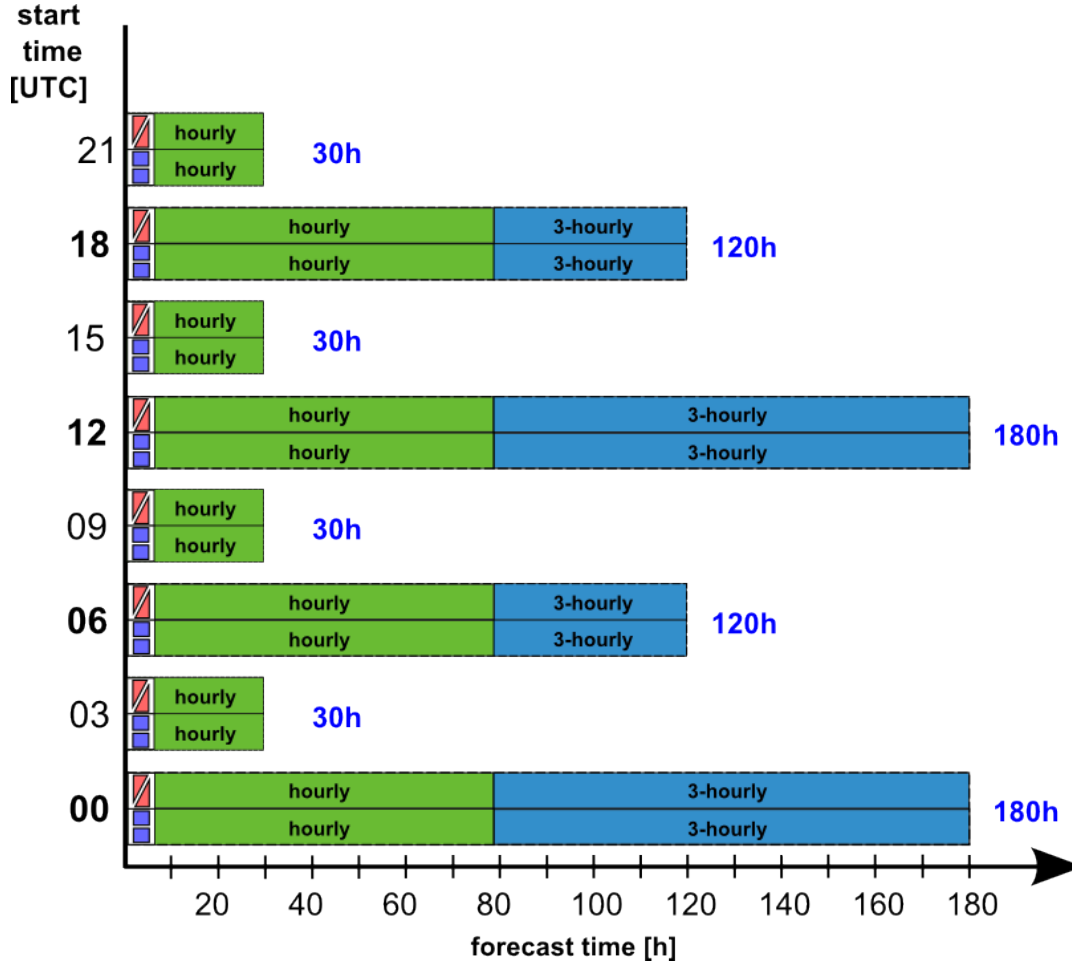


Figure 6.1.: Time span covered by the various global ICON forecasts which are launched every three hours. Output on the native (triangular) grid (▤) and the regular grid (▥) is generally available until forecast end, as indicated by the length of the two bars shown for each forecast run. Output fields are available hourly up to $VV = 78$ h and 3-hourly for larger forecast times.




for the 0 and 12 UTC runs and 120 h for the 6 and 18 UTC runs. Prior to 2015-02-25 the 6 and 18 UTC runs were restricted to 78 h. In preparation for the replacement of COSMO-EU by a high resolution ICON nest, additional short-range forecasts are performed at 3, 9, 15 and 21 UTC. The ICON nest will provide boundary data for the high resolution COSMO-DE runs, once COSMO-EU has been switched off later this year. The forecast time covered by these runs is limited to 30 h. See Chapter 7 for more details on the ICON nest and the available output fields.

All time-dependent output fields are available hourly up to $VV = 78$ h and 3-hourly for larger forecast times². Please note that for ICON fields the time unit is minutes rather than hours, and thus differs from GME (hours).

Output is available on two distinct horizontal grids:

- The native triangular grid with an average resolution of 13 km, and
- a regular latitude-longitude grid with a resolution of $\Delta\lambda = \Delta\Phi = 0.25^\circ$.

On the native grid most output fields are defined on triangle cell (circum-)centers, except for VN , which is defined on cell edges. On the lat-lon grid, all fields are defined on cell centers. A single 2D GRIB2 field on the native and regular lat-lon grid contains 2949120 and 1038240 (721×1440) grid points, respectively.

For details regarding the available fields, please see the tables below. Note that the vertical rules in the leftmost column indicate whether the field is available on the native grid () , on the lat-lon grid() , or on both grids() .









For details regarding the algorithm for interpolation onto the lat-lon grid, see Section 10.2. In the tables below, the specific algorithm used for lat-lon interpolation is indicated in the column **LL IntpType**. If nothing is specified, then an RBF-based interpolation method is used.

6.3.1. Time-constant (external parameter) fields

Table 6.2 provides an overview of the available time invariant fields. They are available from the database category `CAT_NAME=$model_const_an_$suite`. As mentioned in Section 4.2, `DEPTH_LK`, `HSURF`, `FR_LAND`, `FR_LAKE` and `Z0` are modified by `ICON`. Thus, the latter should not be taken from the `const_an` database category, unless you definitely know what you are doing. For convenience, the modified invariant fields (and some more) are stored in the `forecast` database categories for step $s[h] = 0$ (`CAT_NAME=$model_$run_fc_$suite`). Table 6.3 provides a list of all fields which are exclusively written for $s[h] = 0$.

See Section 11.1 for more details on the database categories and Section 11.2 for sample retrievals.

Table 6.2.: Time-constant fields (`CAT_NAME=$model_const_an_$suite`)

| ShortName | Description | Discipline Category Number | Lev-Typ 1/2 | stepType | LL IntpType | Unit |
|--|--|----------------------------------|-------------|----------|-------------|--------|
| Date/Time (YYYY-MM-DDThh) D=0001-01-01T00 | | | | | | |
|  CLAT | Geographical latitude of native grid triangle cell center | 0/191/1 | 1/– | inst | – | Deg. N |
|  CLON | Geographical longitude of native grid triangle cell center | 0/191/2 | 1/– | inst | – | Deg. E |
|  DEPTH_LK | Lake depth | 1/2/0 | 1/162 | inst | – | m |
|  EMIS_RAD | Longwave surface emissivity | 2/3/199 | 1/– | inst | – | 1 |
|  FOR_D | Fraction of deciduous forest (possible range [0, 1]) | 2/0/30 | 1/– | inst | – | 1 |
|  FOR_E | Fraction of evergreen forest (possible range [0, 1]) | 2/0/29 | 1/– | inst | – | 1 |
|  FR_LAKE | Fresh water lake fraction (possible range [0, 1]) | 1/2/2 | 1/– | inst | – | 1 |
|  FR_LAND | Land fraction (possible range [0, 1]) | 2/0/0 | 1/– | inst | – | 1 |

Continued on next page

²An exception here are the output fields `VMAX_10M`, `U_10M` and `V_10M`, which are available hourly throughout the forecast. For the latter two this is because `U_10M` and `V_10M` are needed as input by the wave models.

Table 6.2.: *continued*







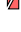



| | | | | | | |
|--|--|----------|-------|------|---|-------------------|
| FR_LUC | Land use class fraction (possible range [0, 1]) | 2/0/36 | 1/– | inst | – | 1 |
| HSURF | Geometric height of the earth's surface above msl | 0/3/6 | 1/101 | inst | – | m |
| LAI_MX | Leaf area index in the vegetation phase | 2/0/28 | 1/– | max | – | 1 |
| NDVI_MAX | Normalized differential vegetation index | 2/0/31 | 1/– | max | – | 1 |
| PLCOV_MX | Plant covering degree in the vegetation phase | 2/0/4 | 1/– | max | – | 1 |
| ROOTDP | Root depth of vegetation | 2/0/32 | 1/– | inst | – | m |
| RSMIN | Minimum stomatal resistance | 2/0/16 | 1/– | inst | – | s m^{-1} |
| SOILTYP | Soil type of land fraction (9 types [1, ..., 9]) | 2/3/196 | 1/– | inst | – | 1 |
| SSO_GAMMA | Anisotropy of sub-gridscale orography | 0/3/24 | 1/– | inst | – | 1 |
| SSO_SIGMA | Slope of sub-gridscale orography | 0/3/22 | 1/– | inst | – | 1 |
| SSO_STDH | Standard deviation of sub-grid scale orography | 0/3/20 | 1/– | inst | – | m |
| SSO_THETA | Angle of sub-gridscale orography | 0/3/21 | 1/– | inst | – | rad |
| T_2M_CL | Climatological 2m temperature (used as lower bc. for soil model) | 0/0/0 | 103/– | inst | – | K |
| Z0 | Surface roughness length (over land) | 2/0/1 | 1/– | inst | – | m |
| Date/Time (YYYY-MM-DDThh) D=1111-01-11T11 | | | | | | |
| AER_SS12 | Sea salt aerosol climatology (monthly fields) | 0/20/102 | 1/– | avg | – | 1 |
| AER_DUST12 | Total soil dust aerosol climatology (monthly fields) | 0/20/102 | 1/– | avg | – | 1 |
| AER_ORG12 | Organic aerosol climatology (monthly fields) | 0/20/102 | 1/– | avg | – | 1 |
| AER_SO412 | Total sulfate aerosol climatology (monthly fields) | 0/20/102 | 1/– | avg | – | 1 |
| AER_BC12 | Black carbon aerosol climatology (monthly fields) | 0/20/102 | 1/– | avg | – | 1 |

Continued on next page

Table 6.2.: *continued*







| | | | | | | | |
|---|-----------|---|----------|-----|-----|---|---|
|  | ALB_DIF12 | Shortwave ($0.3 - 5.0 \mu\text{m}$) albedo for diffuse radiation (monthly fields) | 0/19/18 | 1/– | avg | – | 1 |
|  | ALB_UV12 | UV-visible ($0.3 - 0.7 \mu\text{m}$) albedo for diffuse radiation (monthly fields) | 0/19/222 | 1/– | avg | – | 1 |
|  | ALB_NI12 | Near infrared ($0.7 - 5.0 \mu\text{m}$) albedo for diffuse radiation (monthly fields) | 0/19/223 | 1/– | avg | – | 1 |
|  | NDVI_MRAT | ratio of monthly mean NDVI (normalized differential vegetation index) to annual max | 0/0/192 | 1/– | avg | – | 1 |

Table 6.3.: Variables exclusively available for $VV = 0$ from the forecast databases (CAT_NAME=\$model_\$run_fc_\$suite, $s[h] = 0$)

| ShortName | Description | Discipline Category Number | Lev-Typ 1/2 | stepType | LL IntpType | Unit |
|--|--|----------------------------------|-------------|----------|-------------|--------|
|  CLAT | Geographical latitude of native grid triangle cell center | 0/191/1 | 1/– | inst | – | Deg. N |
|  CLON | Geographical longitude of native grid triangle cell center | 0/191/2 | 1/– | inst | – | Deg. E |
|  DEPTH_LK | Lake depth | 1/2/0 | 1/162 | inst | | m |
|  ELAT | Geographical latitude of native grid triangle edge midpoint | 0/191/1 | 1/– | inst | – | Deg. N |
|  ELON | Geographical longitude of native grid triangle edge midpoint | 0/191/2 | 1/– | inst | – | Deg. E |
|  FR_LAKE | Fresh water lake fraction (possible range [0, 1]) | 1/2/2 | 1/– | inst | | 1 |
|  FR_LAND | Land fraction (possible range [0, 1]) | 2/0/0 | 1/– | inst | | 1 |
|  HHL | Geometric height of model half levels above msl | 0/3/6 | 150/101 | inst | | m |
|  HSURF | Geometric height of the earths surface above msl | 0/3/6 | 1/101 | inst | | m |
|  LAI | Leaf area index | 2/0/28 | 1/– | inst | | 1 |









Continued on next page

Table 6.3.: *continued*

| | | | | | | |
|---|--|---------|-----|------|-----|--------|
|  NDVIRATIO | ratio of current NDVI (normalized differential vegetation index) to annual max | 2/0/192 | 1/– | inst | – | 1 |
|  PLCOV | Plant cover | 2/0/4 | 1/– | inst | | % |
|  RLAT | Geographical latitude of regular lat-lon grid cell centers | 0/191/1 | 1/– | inst | | Deg. N |
|  RLON | Geographical longitude of regular lat-lon grid cell centers | 0/191/2 | 1/– | inst | | Deg. E |
|  ROOTDP | Root depth of vegetation | 2/0/32 | 1/– | inst | | m |
|  SOILTYP | Soil type of land fraction (9 types [1, ..., 9]) | 2/3/196 | 1/– | inst | NNB | 1 |








6.3.2. Multi-level fields on native hybrid vertical levels

Table 6.4.: Hybrid multi-level forecast ($VV > 0$) and initialised analysis ($VV = 0$) products

| ShortName | Description | Discipline Category Number | Lev-Typ 1/2 | stepType | LL IntpType | Unit |
|--|---|----------------------------------|-------------|----------|-------------|--------------------------------|
|  CLC | Cloud cover | 0/6/22 | 150/150 | inst | | % |
|  DEN | Density of moist air | 0/3/10 | 150/150 | inst | – | kg m ⁻³ |
|  DTKE_CON | Buoyancy-production of TKE due to sub grid scale convection | 0/19/219 | 150/– | inst | – | m ² s ⁻³ |
|  DTKE_HSH | Production of TKE due to horizontal shear | 0/19/220 | 150/– | inst | – | m ² s ⁻³ |
|  P | Pressure | 0/3/0 | 150/150 | inst | | Pa |
|  QC | Cloud mixing ratio ³ | 0/1/22 | 150/150 | inst | | kg kg ⁻¹ |
|  QI | Cloud ice mixing ratio ³ | 0/1/82 | 150/150 | inst | | kg kg ⁻¹ |
|  QR | Rain mixing ratio ³ | 0/1/24 | 150/150 | inst | – | kg kg ⁻¹ |

Continued on next page

Table 6.4.: *continued*

| | | | | | | |
|---|--------------------------------|---------|---------|------|---|--------------------------------|
|  QS | Snow mixing ratio ³ | 0/1/25 | 150/150 | inst | – | kg kg ⁻¹ |
|  QV | Specific humidity | 0/1/0 | 150/150 | inst | | kg kg ⁻¹ |
|  T | Temperature | 0/0/0 | 150/150 | inst | | K |
|  TKE | Turbulent kinetic energy | 0/19/11 | 150/– | inst | | m ² s ⁻² |
|  U | Zonal wind | 0/2/2 | 150/150 | inst | | m s ⁻¹ |
|  V | Meridional wind | 0/2/3 | 150/150 | inst | | m s ⁻¹ |
|  W | Vertical wind | 0/2/9 | 150/– | inst | | m s ⁻¹ |

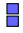
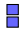
6.3.3. Multi-level fields interpolated to pressure levels

For regular grid output the following 36 pressure levels are available:

1000, 975, 950, 925, 900, 875, 850, 825, 800, 775,
 750, 700, 650, 600, 550, 500, 450, 400, 350, 300,
 275, 250, 225, 200, 175, 150, 125, 100, 70, 50, 30,
 10, 5, **2**, **1**, **0.1** hPa.

The output fields are listed in Table 6.5. Note that the fields CLC, OMEGA, and RELHUM are only available from 1000 hPa down to 5 hPa, i.e. they are not available on the levels highlighted in **blue**.

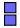
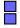
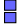
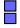
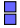
Table 6.5.: Regular grid output: Multi-level forecast ($VV > 0$) and initialised analysis ($VV = 0$) products interpolated to pressure levels 1000, 975, 950, 925, 900, 875, 850, 825, 800, 775, 750, 700, 650, 600, 550, 500, 450, 400, 350, 300, 275, 250, 225, 200, 175, 150, 125, 100, 70, 50, 30, 10, 5, **2**, **1**, **0.1** hPa. The fields CLC, OMEGA, and RELHUM are not available for the pressure levels highlighted in **blue**.

| ShortName | Description | Discipline Category Number | Lev-Typ 1/2 | stepType | LL IntpType | Unit |
|---|--------------|----------------------------------|-------------|----------|-------------|--------------------------------|
|  CLC | Cloud cover | 0/6/22 | 100/– | inst | | % |
|  FI | Geopotential | 0/3/4 | 100/– | inst | | m ² s ⁻² |

Continued on next page

³for the time being, erroneously encoded as mixing ratios instead of specific quantities

Table 6.5.: *continued*






| | | | | | |
|--|--|-------|-------|------|--------------------|
|  OMEGA | Vertical velocity in pressure coordinates ($\omega = dp/dt$) | 0/2/8 | 100/- | inst | Pa s^{-1} |
|  RELHUM | Relative humidity (with respect to water) | 0/1/1 | 100/- | inst | % |
|  T | Temperature | 0/0/0 | 100/- | inst | K |
|  U | Zonal wind | 0/2/2 | 100/- | inst | m s^{-1} |
|  V | Meridional wind | 0/2/3 | 100/- | inst | m s^{-1} |

On the native (triangular) grid, output is generated for levels

1000, 950, 850, 700, 500, 300 hPa.



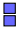













The output fields are listed in Table 6.6.

Table 6.6.: Native (triangular) grid output: Multi-level forecast ($VV > 0$) and initialised analysis ($VV = 0$) products interpolated to pressure levels 1000, 950, 850, 700, 500, 300 hPa.

| ShortName | Description | Discipline Category Number | Lev-Typ 1/2 | stepType | LL IntpType | Unit |
|--|---|----------------------------------|-------------|----------|-------------|----------------------------|
|  FI | Geopotential | 0/3/4 | 100/- | inst | - | $\text{m}^2 \text{s}^{-2}$ |
|  RELHUM | Relative humidity (with respect to water) | 0/1/1 | 100/- | inst | - | % |
|  T | Temperature | 0/0/0 | 100/- | inst | - | K |
|  U | Zonal wind | 0/2/2 | 100/- | inst | - | m s^{-1} |
|  V | Meridional wind | 0/2/3 | 100/- | inst | - | m s^{-1} |






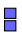










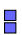



6.3.4. Single-level fields

Table 6.7.: Single-level forecast ($VV > 0$) and initialised analysis ($VV = 0$) products

| ShortName | Description | Discipline Category Number | Lev-Typ 1/2 | stepType | LL IntpType | Unit |
|---|--|----------------------------------|-------------|----------|-------------|--------------------|
|  ALB_RAD | Shortwave broadband albedo for diffuse radiation | 0/19/1 | 1/– | inst | | % |
|  ALHFL_S | Latent heat net flux at surface (average since model start) | 0/0/10 | 1/– | avg | | W m^{-2} |
|  APAB_S | Photosynthetically active radiation flux at surface (average since model start) | 0/4/10 | 1/– | avg | | W m^{-2} |
|  ASHFL_S | Sensible heat net flux at surface (average since model start) | 0/0/11 | 1/– | avg | | W m^{-2} |
|  ASOB_S | Net short-wave radiation flux at surface (average since model start) | 0/4/9 | 1/– | avg | | W m^{-2} |
|  ASOB_T | Net short-wave radiation flux at top of atmosphere (TOA) (average since model start) | 0/4/9 | 8/– | avg | | W m^{-2} |
|  ASWDIFD_S | Surface down solar diffuse radiation (average since model start) | 0/4/199 | 1/– | avg | | W m^{-2} |
|  ASWDIFU_S | Surface up solar diffuse radiation (average since model start) | 0/4/8 | 1/– | avg | | W m^{-2} |
|  ASWDIR_S | Surface down solar direct radiation (average since model start) | 0/4/198 | 1/– | avg | | W m^{-2} |
|  ATHB_S | Net long-wave radiation flux at surface (average since model start) | 0/5/5 | 1/– | avg | | W m^{-2} |
|  ATHB_T | Net long-wave radiation flux at TOA (average since model start) | 0/5/5 | 8/– | avg | | W m^{-2} |
|  AUMFL_S | U-momentum flux at surface $\frac{u'w'}{w'^{1/2}}$ (average since model start) | 0/2/17 | 1/– | avg | | m |
|  AVMFL_S | V-momentum flux at surface $\frac{v'w'}{w'^{1/2}}$ (average since model start) | 0/2/18 | 1/– | avg | | m |
|  CAPE_CON | Convective available potential energy | 0/7/6 | 1/– | inst | – | J kg^{-1} |
|  CAPE_ML | Mixed layer CAPE | 0/7/6 | 192/– | inst | NNB | J kg^{-1} |
|  CIN_ML | Mixed layer convective inhibition | 0/7/7 | 192/– | inst | NNB | J kg^{-1} |




















Continued on next page

Table 6.7.: *continued*

| | | | | | | |
|---|--|---------|---------|------|-----|---------------------|
|  CLCH | High level clouds | 0/6/22 | 100/100 | inst | | % |
|  CLCM | Mid level clouds | 0/6/22 | 100/100 | inst | | % |
|  CLCL | Low level clouds | 0/6/22 | 100/1 | inst | | % |
|  CLCT | Total cloud cover | 0/6/1 | 1/– | inst | | % |
|  CLCT_MOD | Modified total cloud cover for media | 0/6/199 | 1/– | inst | | 1 |
|  CLDEPTH | Modified cloud depth for media | 0/6/198 | 1/– | inst | | 1 |
|  FRESHSNW | Fresh snow factor (weighting function for albedo indicating freshness of snow) | 0/1/203 | 1/– | inst | – | 1 |
|  FR_ICE | Sea/lake ice cover (possible range: [0, 1]) | 10/2/0 | 1/– | inst | | 1 |
|  HBAS_CON | Height of convective cloud base above msl | 0/6/26 | 2/101 | inst | NNB | m |
|  H_ICE | Sea/Lake ice thickness (Max: 3 m) | 10/2/1 | 1/– | inst | | m |
|  H_SNOW | Snow depth | 0/1/11 | 1/– | inst | | m |
|  HTOP_CON | Height of convective cloud top above msl | 0/6/27 | 3/101 | inst | NNB | m |
|  HTOP_DC | Height of top of dry convection above msl | 0/6/196 | 3/101 | inst | NNB | m |
|  HZEROCL | Height of 0 degree Celsius isotherm above msl | 0/3/6 | 4/101 | inst | NNB | m |
|  PMSL | Surface pressure reduced to msl | 0/3/1 | 101/– | inst | | Pa |
|  PS | Surface pressure (not reduced) | 0/3/0 | 1/– | inst | | Pa |
|  QV_2M | Specific humidity at 2m above ground | 0/1/0 | 103/– | inst | | kg kg ⁻¹ |
|  QV_S | Surface specific humidity | 0/1/0 | 1/– | inst | | kg kg ⁻¹ |
|  RAIN_CON ⁴ | Convective rain (accumulated since model start) | 0/1/76 | 1/– | accu | BCT | kg m ⁻² |
|  RAIN_GSP ⁴ | Large scale rain (accumulated since model start) | 0/1/77 | 1/– | accu | BCT | kg m ⁻² |















Continued on next page

Table 6.7.: *continued*

| | | | | | | |
|---|---|---------|-------|------|-----|--------------------|
|  RELHUM_2M | Relative humidity at 2m above ground | 0/1/1 | 103/– | inst | | % |
|  RHO_SNOW | Snow density | 0/1/61 | 1/– | inst | | kg m ⁻³ |
|  RUNOFF_G | Soil water runoff (accumulated since model start) | 2/0/5 | 106/– | accu | | kg m ⁻² |
|  RUNOFF_S | Surface water runoff (accumulated since model start) | 2/0/5 | 106/– | accu | | kg m ⁻² |
|  SNOW_CON ⁴ | Convective snowfall water equivalent (accumulated since model start) | 0/1/55 | 1/– | accu | BCT | kg m ⁻² |
|  SNOW_GSP ⁴ | Large snowfall water equivalent (accumulated since model start) | 0/1/56 | 1/– | accu | BCT | kg m ⁻² |
|  SOBS_RAD | Net short-wave radiation flux at surface (instantaneous) | 0/4/9 | 1/– | inst | | W m ⁻² |
|  T_2M | Temperature at 2m above ground | 0/0/0 | 103/– | inst | | K |
|  TCH | Turbulent transfer coefficient for heat and moisture (surface) | 0/0/19 | 1/– | inst | | 1 |
|  TCM | Turbulent transfer coefficient for momentum (surface) | 0/2/29 | 1/– | inst | | 1 |
|  TD_2M | Dew point temperature at 2m above ground | 0/0/6 | 103/– | inst | | K |
|  T_G | Ground temperature (temperature at sfc-atm interface) | 0/0/0 | 1/– | inst | | K |
|  THBS_RAD | Net long-wave radiation flux at surface (instantaneous) | 0/5/5 | 1/– | inst | | W m ⁻² |
|  T_ICE | Sea/Lake ice temperature (at ice-atm interface) | 10/2/8 | 1/– | inst | | K |
|  TMAX_2M | Maximum temperature at 2m above ground | 0/0/0 | 103/– | max | | K |
|  TMIN_2M | Minimum temperature at 2m above ground | 0/0/0 | 103/– | min | | K |
|  TOT_PREC ⁴ | Total precipitation (accumulated since model start) | 0/1/52 | 1/– | accu | BCT | kg m ⁻² |
|  TQC | Column integrated cloud water (grid scale) | 0/1/69 | 1/– | inst | | kg m ⁻² |
|  TQC_DIA | Total column integrated cloud water (including sub-grid-scale contribution) | 0/1/215 | 1/– | inst | | kg m ⁻² |

Continued on next page

Table 6.7.: *continued*

| | | | | | | |
|--|---|---------|-------|------|-----|--------------------|
|  TQI | Column integrated cloud ice (grid scale) | 0/1/70 | 1/– | inst | | kg m ⁻² |
|  TQI_DIA | Total column integrated cloud ice (including sub-grid-scale contribution) | 0/1/216 | 1/– | inst | | kg m ⁻² |
|  TQR | Column integrated rain (grid scale) | 0/1/45 | 1/– | inst | | kg m ⁻² |
|  TQS | Column integrated snow (grid scale) | 0/1/46 | 1/– | inst | | kg m ⁻² |
|  TQV | Column integrated water vapour (grid scale) | 0/1/64 | 1/– | inst | | kg m ⁻² |
|  T_S ⁵ | Temperature of the soil surface (equivalent to T_SO(0)) | 2/3/18 | 1/– | inst | | K |
|  T_SNOW | Temperature of the snow surface | 0/0/18 | 1/– | inst | | K |
|  U_10M | Zonal wind at 10m above ground | 0/2/2 | 103/– | inst | | m s ⁻¹ |
|  V_10M | Meridional wind at 10m above ground | 0/2/3 | 103/– | inst | | m s ⁻¹ |
|  VMAX_10M | Maximum wind at 10 m above ground | 0/2/22 | 103/– | max | | m s ⁻¹ |
|  W_I | Plant canopy surface water | 2/0/13 | 1/– | inst | – | kg m ⁻² |
|  W_SNOW | Snow depth water equivalent | 0/1/60 | 1/– | inst | | kg m ⁻² |
|  WW | Weather interpretation (WMO), see Table 6.8 for details. | 0/19/25 | 1/– | inst | NNB | 1 |
|  Z0 | Surface roughness (above land and water) | 2/0/1 | 1/– | inst | | m |

⁴Note that the unit which is displayed, when inspecting the GRIB2 message with *grib_dump* is kg m⁻² s⁻¹ rather than kg m⁻². Mathematically this is wrong, however, it is in accordance with the GRIB2 standard. To get the mathematically correct unit for accumulated fields (*typeOfStatisticalProcessing*=1), the unit displayed by *grib_dump* must be multiplied by s.

⁵T_S is identical to T_SO at level 0. It will no longer be available in the future. Use T_SO(0) instead of T_S.

| WW | weather interpretation | WW | weather interpretation |
|----|---|----|-----------------------------------|
| 45 | Fog | 48 | Fog, depositing rime |
| 50 | Slight drizzle | 56 | Drizzle, freezing, slight |
| 60 | Slight rain, not freezing | 63 | Moderate rain, not freezing |
| 65 | Heavy rain, not freezing | 66 | Rain, freezing, slight |
| 67 | Rain, freezing, moderate or heavy | 70 | Slight fall of snowflakes |
| 73 | Moderate fall of snowflakes | 75 | Heavy fall of snowflakes |
| 80 | Rain shower(s), slight | 81 | Rain shower(s), moderate or heavy |
| 82 | Rain shower(s), violent | 85 | Snow shower(s), slight |
| 86 | Snow shower(s), moderate or heavy | 95 | Thunderstorm, slight or moderate |
| 96 | Thunderstorm with hail, or heavy thunderstorm | | |

Table 6.8.: Weather interpretation (WW) code table for the ICON model. This table is a subset of the WMO code table *FM 94 BUFR/FM 95 CREX code table 0 20 003 – present weather*. In the case that none of the values provided in Table 6.8 is returned, the WW output contains the total cloud cover, encoded in the following form: **0**: clear sky **1**: mainly clear **2**: partly/generally cloudy **3**: cloudy/overcast.

6.3.5. Soil-specific multi-level fields

Table 6.9.: Multi-level forecast ($VV > 0$) and initialised analysis ($VV = 0$) products of the soil model

| ShortName | Description | Discipline Category Number | Lev-Typ 1/2 | stepType | LL IntpType | Unit |
|--|---|----------------------------------|-------------|----------|-------------|--------------------|
|  T_SO | Soil temperature | 2/3/18 | 106/- | inst | | K |
|  W_SO | Soil moisture integrated over individual soil layers (ice + liquid) | 2/3/20 | 106/106 | inst | | kg m ⁻² |
|  W_SO_ICE | Soil ice content integrated over individual soil layers | 2/3/22 | 106/106 | inst | NNB | kg m ⁻² |

Soil temperature is defined at the soil depths given in Table 6.10 (column 2). Levels 1 to 8 define the full levels of the soil model. A zero gradient condition is assumed between levels 0 and 1, meaning that temperatures at the surface-atmosphere interface are set equal to the temperature at the first full level depth. (0.5 cm). Temperatures are prognosed for layers 1 to 7. At the lowermost layer (mid-level height 1458 cm) the temperature is fixed to the climatological average 2 m-temperature.

Soil moisture W_SO is prognosed for layers 1 to 6. In the two lowermost layers W_SO is filled with W_SO(6) (zero gradient condition).

Table 6.10.: Soil model: vertical distribution of levels and layers

| level no. | depth [cm] | layer no. | upper/lower bounds [cm] |
|-----------|------------|-----------|-------------------------|
| 0 | 0.0 | | |
| 1 | 0.5 | 1 | 0.0 — 1.0 |
| 2 | 2.0 | 2 | 1.0 — 3.0 |
| 3 | 6.0 | 3 | 3.0 — 9.0 |
| 4 | 18.0 | 4 | 9.0 — 27.0 |
| 5 | 54.0 | 5 | 27.0 — 81.0 |
| 6 | 162.0 | 6 | 81.0 — 243.0 |
| 7 | 486.0 | 7 | 243.0 — 729.0 |
| 8 | 1458.0 | 8 | 729.0 — 2187.0 |

6.3.6. Lake-specific single-level fields

Table 6.11.: Single-level forecast ($VV > 0$) and initialised analysis ($VV = 0$) products of the lake model model

| ShortName | Description | Discipline Category Number | Lev-Typ 1/2 | stepType | LL IntpType | Unit |
|------------|---|----------------------------------|-------------|----------|-------------|------|
| ▣ C_T_LK | Shape factor with respect to the temperature profile in the thermocline | 1/2/10 | 162/166 | inst | — | 1 |
| ▣ H_ML_LK | Mixed-layer depth | 1/2/0 | 1/166 | inst | — | m |
| ▣ T_BOT_LK | Temperature at the water-bottom sediment interface | 1/2/1 | 162/— | inst | — | K |
| ▣ T_MNW_LK | Mean temperature of the water column | 1/2/1 | 1/162 | inst | — | K |
| ▣ T_WML_LK | Mixed-layer temperature | 1/2/1 | 1/166 | inst | — | K |

7. EU Nest output fields: Forecast runs

7.1. Available output fields




This section contains a list of output fields that are available with the launch of the ICON-EU nest. See Fig. 3.6a on page 10 for details regarding the nest location and extent. Forecasts on the EU-nest are performed multiple times a day with varying forecast periods. Forecasts reaching out to 120 h are performed at 00, 06, 12, and 18 UTC. Additional short-range forecasts reaching out to 30 h are performed at 03, 09, 15 and 21 UTC. Its main purpose is to provide boundary data for the high resolution COSMO-DE runs. A schematic overview of the various forecasts, including its forecast period and output intervals is provided in Figure 7.1.

Output is available on two distinct horizontal grids:

- a native triangular grid with an average resolution of 6.5 km, and
- a regular latitude-longitude grid with a resolution of $\Delta\lambda = \Delta\Phi = 0.0625^\circ$.

See Table 7.1 for a summary.

Output on the native (triangular) grid is hourly to 48 h, and every 6 hours for verification until the forecast end at 120 h. Output on the regular grid is hourly to 78 h, and every 3 hours until forecast end. See also Figure 7.1.

Again, in the subsequent tables the availability of specific fields on the native grid () , on the lat-lon grid() , or on both grids () is marked in the leftmost column. The method used for lat-lon interpolation is indicated in the column LL IntpType.

| | global lat-lon | EU nest lat-lon |
|--------------------|-------------------------------------|---|
| geogr. coordinates | 0.0° – 359.75° 90.0° S – 90.0° N | 23.5° W – 62.5° E, 29.5° N – 70.5° N |
| mesh size | 0.25° | 0.0625° |

Table 7.1.: Summary of the latitude-longitude grids for ICON global and ICON-EU nest output.

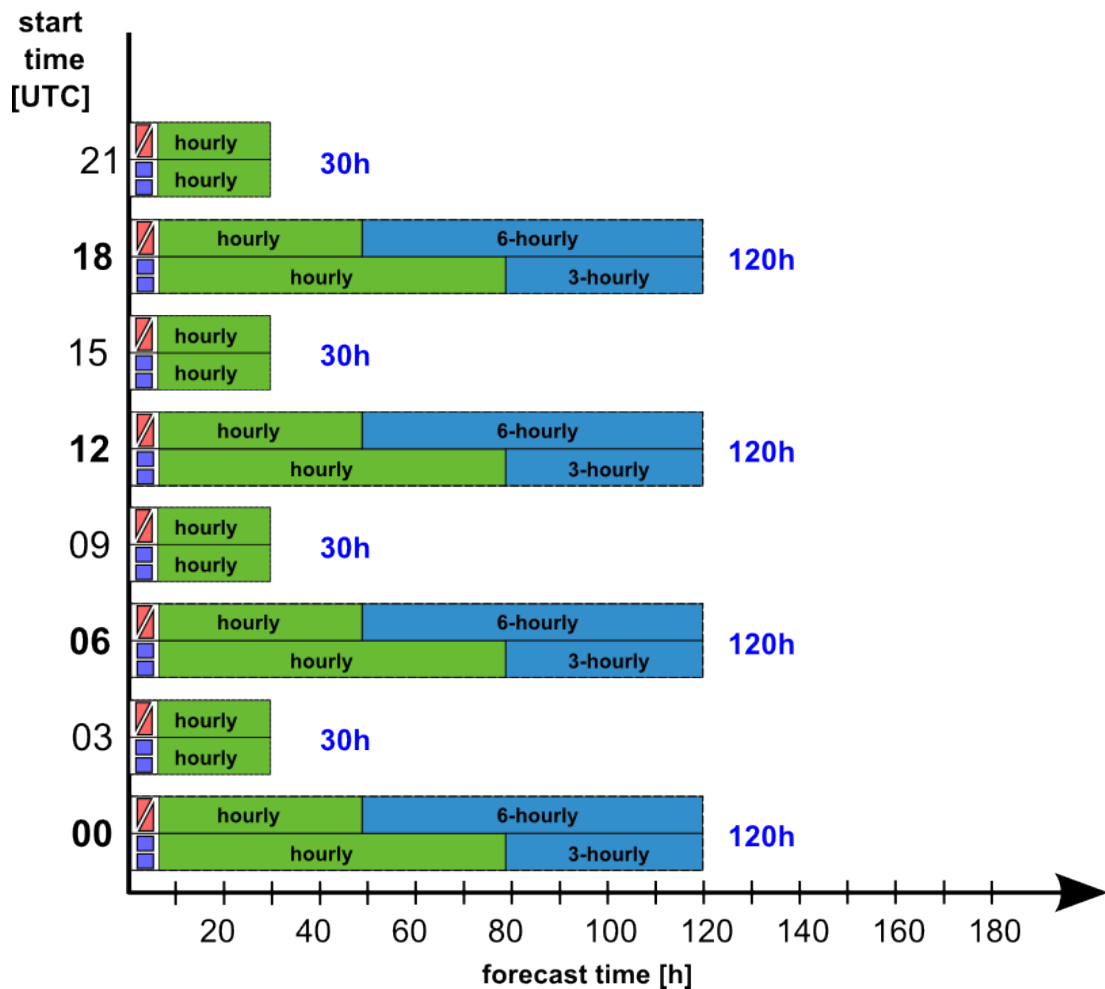


Figure 7.1.: Time span covered by the various EU nest forecasts which are launched every three hours. Output on the native (triangular) grid (▨) and the regular grid (▩) is generally available until forecast end, as indicated by the length of the two bars shown for each forecast run. Output on the native grid is available hourly to 48 h, and every 6 hours for later forecast times. Output on the regular grid is available hourly to 78 h, and every 3 hours for later forecast times.

7.1.1. Time-constant (external parameter) fields for the EU nest

Table 7.2.: Variables exclusively available for $VV = 0$ from the forecast databases (CAT_NAME=\$model_\$run_fc_\$suite, $s[h] = 0$)

| ShortName | Description | Discipline Category Number | Lev-Typ 1/2 | stepType | LL IntpType | Unit |
|-----------|---|----------------------------------|-------------|----------|-------------|--------|
| ▨ CLAT | Geographical latitude of native grid triangle cell center | 0/191/1 | 1/- | inst | - | Deg. N |












Continued on next page

Table 7.2.: *continued*

| | | | | | | |
|---|--|---------|---------|------|-----|--------|
|  CLON | Geographical longitude of native grid triangle cell center | 0/191/2 | 1/– | inst | – | Deg. E |
|  DEPTH_LK | Lake depth | 1/2/0 | 1/162 | inst | | m |
|  ELAT | Geographical latitude of native grid triangle edge midpoint | 0/191/1 | 1/– | inst | – | Deg. N |
|  ELON | Geographical longitude of native grid triangle edge midpoint | 0/191/2 | 1/– | inst | – | Deg. E |
|  FR_LAKE | Fresh water lake fraction (possible range [0, 1]) | 1/2/2 | 1/– | inst | | 1 |
|  FR_LAND | Land fraction (possible range [0, 1]) | 2/0/0 | 1/– | inst | | 1 |
|  HHL | Geometric height of model half levels above msl | 0/3/6 | 150/101 | inst | | m |
|  HSURF | Geometric height of the earths surface above msl | 0/3/6 | 1/101 | inst | | m |
|  LAI | Leaf area index | 2/0/28 | 1/– | inst | | 1 |
|  PLCOV | Plant cover | 2/0/4 | 1/– | inst | | % |
|  RLAT | Geographical latitude of regular lat-lon grid cell centers | 0/191/1 | 1/– | inst | | Deg. N |
|  RLON | Geographical longitude of regular lat-lon grid cell centers | 0/191/2 | 1/– | inst | | Deg. E |
|  ROOTDP | Root depth of vegetation | 2/0/32 | 1/– | inst | | m |
|  SOILTYP | Soil type of land fraction (9 types [1, ..., 9]) | 2/3/196 | 1/– | inst | NNB | 1 |

7.1.2. Multi-level fields on native hybrid vertical levels for the EU nest

Table 7.3.: Hybrid multi-level forecast ($VV > 0$) and initialised analysis ($VV = 0$) products

| ShortName | Description | Discipline Category Number | Lev-Typ 1/2 | stepType | LL IntpType | Unit |
|--|---|----------------------------------|-------------|----------|-------------|----------------------------|
|  CLC | Cloud cover | 0/6/22 | 150/150 | inst | | % |
|  DTKE_CON | Buoyancy-production of TKE due to sub grid scale convection | 0/19/219 | 150/- | inst | - | $\text{m}^2 \text{s}^{-3}$ |
|  DTKE_HSH | Production of TKE due to horizontal shear | 0/19/220 | 150/- | inst | - | $\text{m}^2 \text{s}^{-3}$ |
|  P | Pressure | 0/3/0 | 150/150 | inst | | Pa |
|  QC | Cloud mixing ratio ³ | 0/1/22 | 150/150 | inst | | kg kg^{-1} |
|  QI | Cloud ice mixing ratio ³ | 0/1/82 | 150/150 | inst | | kg kg^{-1} |
|  QR | Rain mixing ratio ³ | 0/1/24 | 150/150 | inst | - | kg kg^{-1} |
|  QS | Snow mixing ratio ³ | 0/1/25 | 150/150 | inst | - | kg kg^{-1} |
|  QV | Specific humidity | 0/1/0 | 150/150 | inst | | kg kg^{-1} |
|  T | Temperature | 0/0/0 | 150/150 | inst | | K |
|  TKE | Turbulent kinetic energy | 0/19/11 | 150/- | inst | | $\text{m}^2 \text{s}^{-2}$ |
|  U | Zonal wind | 0/2/2 | 150/150 | inst | | m s^{-1} |
|  V | Meridional wind | 0/2/3 | 150/150 | inst | | m s^{-1} |
|  W | Vertical wind | 0/2/9 | 150/- | inst | | m s^{-1} |

²for the time being, erroneously encoded as mixing ratios instead of specific quantities

7.1.3. Multi-level fields interpolated to pressure levels

For regular grid output the following 30 pressure levels are available:

1000, 975, 950, 925, 900, 875, 850, 825, 800, 775,
750, 700, 650, 600, 550, 500, 450, 400, 350, 300,
275, 250, 225, 200, 175, 150, 125, 100, 70, 50 hPa.

The output fields are listed in Table 7.4.

On the native (triangular) grid no output is generated for pressure levels.

Table 7.4.: Regular grid output on the ICON EU Nest: Multi-level forecast ($VV > 0$) and initialised analysis ($VV = 0$) products interpolated to pressure levels 1000, 975, 950, 925, 900, 875, 850, 825, 800, 775, 750, 700, 650, 600, 550, 500, 450, 400, 350, 300, 275, 250, 225, 200, 175, 150, 125, 100, 70, 50 hPa.

| ShortName | Description | Discipline Category Number | Lev-Typ 1/2 | stepType | LL IntpType | Unit |
|-----------|---|----------------------------------|-------------|----------|-------------|----------------------------|
| CLC | Cloud cover | 0/6/22 | 100/- | inst | | % |
| FI | Geopotential | 0/3/4 | 100/- | inst | | $\text{m}^2 \text{s}^{-2}$ |
| OMEGA | Vertical velocity in pressure coordinates ($\omega = dp/dt$) | 0/2/8 | 100/- | inst | | Pa s^{-1} |
| RELHUM | Relative humidity (with respect to water) | 0/1/1 | 100/- | inst | | % |
| T | Temperature | 0/0/0 | 100/- | inst | | K |
| U | Zonal wind | 0/2/2 | 100/- | inst | | m s^{-1} |
| V | Meridional wind | 0/2/3 | 100/- | inst | | m s^{-1} |

7.1.4. Single-level fields

Table 7.5.: Single-level forecast ($VV > 0$) and initialised analysis ($VV = 0$) products on the ICON EU Nest

| ShortName | Description | Discipline Category Number | Lev-Typ 1/2 | stepType | LL IntpType | Unit |
|-----------|---|----------------------------------|-------------|----------|-------------|------|
| ALB_RAD | Shortwave broadband albedo for diffuse radiation | 0/19/1 | 1/- | inst | | % |

Continued on next page

Table 7.5.: continued

| | | | | | | |
|--|---|---------|---------|------|-----|--------------------|
|  ALHFL_S | Latent heat net flux at surface (average since model start) | 0/0/10 | 1/– | avg | | W m^{-2} |
|  APAB_S | Photosynthetically active radiation flux at surface (average since model start) | 0/4/10 | 1/– | avg | | W m^{-2} |
|  ASHFL_S | Sensible heat net flux at surface (average since model start) | 0/0/11 | 1/– | avg | | W m^{-2} |
|  ASOB_S | Net short-wave radiation flux at surface (average since model start) | 0/4/9 | 1/– | avg | | W m^{-2} |
|  ASOB_T | Net short-wave radiation flux at TOA (average since model start) | 0/4/9 | 8/– | avg | | W m^{-2} |
|  ASWDIFD_S | Surface down solar diffuse radiation (average since model start) | 0/4/199 | 1/– | avg | | W m^{-2} |
|  ASWDIFU_S | Surface up solar diffuse radiation (average since model start) | 0/4/8 | 1/– | avg | | W m^{-2} |
|  ASWDIR_S | Surface down solar direct radiation (average since model start) | 0/4/198 | 1/– | avg | | W m^{-2} |
|  ATHB_S | Net long-wave radiation flux at surface (average since model start) | 0/5/5 | 1/– | avg | | W m^{-2} |
|  ATHB_T | Net long-wave radiation flux at TOA (average since model start) | 0/5/5 | 8/– | avg | | W m^{-2} |
|  AUMFL_S | U-momentum flux at surface $\overline{u'w'}^{1/2}$ (average since model start) | 0/2/17 | 1/– | avg | | m |
|  AVMFL_S | V-momentum flux at surface $\overline{v'w'}^{1/2}$ (average since model start) | 0/2/18 | 1/– | avg | | m |
|  CAPE_CON | Convective available potential energy | 0/7/6 | 1/– | inst | NNB | J kg^{-1} |
|  CAPE_ML | Mixed layer CAPE | 0/7/6 | 192/– | inst | NNB | J kg^{-1} |
|  CIN_ML | Mixed layer convective inhibition | 0/7/7 | 192/– | inst | NNB | J kg^{-1} |
|  CLCH | High level clouds | 0/6/22 | 100/100 | inst | | % |
|  CLCM | Mid level clouds | 0/6/22 | 100/100 | inst | | % |
|  CLCL | Low level clouds | 0/6/22 | 100/1 | inst | | % |
|  CLCT | Total cloud cover | 0/6/1 | 1/– | inst | | % |
|  CLCT_MOD | Modified total cloud cover for media | 0/6/199 | 1/– | inst | | 1 |
|  CLDEPTH | Modified cloud depth for media | 0/6/198 | 1/– | inst | | 1 |





















Continued on next page

Table 7.5.: *continued*

| | | | | | | |
|---|--|---------|-------|------|-----|---------------------|
|  FRESHSNW | Fresh snow factor (weighting function for albedo indicating freshness of snow) | 0/1/203 | 1/– | inst | – | 1 |
|  FR_ICE | Sea/lake ice cover (possible range: [0, 1]) | 10/2/0 | 1/– | inst | – | 1 |
|  HBAS_CON | Height of convective cloud base above msl | 0/6/26 | 2/101 | inst | NNB | m |
|  H_ICE | Sea/Lake ice thickness (Max: 3 m) | 10/2/1 | 1/– | inst | | m |
|  H_SNOW | Snow depth | 0/1/11 | 1/– | inst | | m |
|  HTOP_CON | Height of convective cloud top above msl | 0/6/27 | 3/101 | inst | NNB | m |
|  HTOP_DC | Height of top of dry convection above msl | 0/6/196 | 3/101 | inst | NNB | m |
|  HZEROCL | Height of 0 degree Celsius isotherm above msl | 0/3/6 | 4/101 | inst | NNB | m |
|  PMSL | Surface pressure reduced to msl | 0/3/1 | 101/– | inst | | Pa |
|  PS | Surface pressure (not reduced) | 0/3/0 | 1/– | inst | | Pa |
|  QV_2M | Specific humidity at 2m above ground | 0/1/0 | 103/– | inst | | kg kg ⁻¹ |
|  QV_S | Surface specific humidity | 0/1/0 | 1/– | inst | | kg kg ⁻¹ |
|  RAIN_CON | Convective rain (accumulated since model start) | 0/1/76 | 1/– | accu | BCT | kg m ⁻² |
|  RAIN_GSP | Large scale rain (accumulated since model start) | 0/1/77 | 1/– | accu | BCT | kg m ⁻² |
|  RELHUM_2M | Relative humidity at 2m above ground | 0/1/1 | 103/– | inst | | % |
|  RHO_SNOW | Snow density | 0/1/61 | 1/– | inst | | kg m ⁻³ |
|  RUNOFF_G | Soil water runoff (accumulated since model start) | 2/0/5 | 106/– | accu | | kg m ⁻² |
|  RUNOFF_S | Surface water runoff (accumulated since model start) | 2/0/5 | 106/– | accu | | kg m ⁻² |
|  SNOW_CON | Convective snowfall water equivalent (accumulated since model start) | 0/1/55 | 1/– | accu | BCT | kg m ⁻² |
|  SNOW_GSP | Large snowfall water equivalent (accumulated since model start) | 0/1/56 | 1/– | accu | BCT | kg m ⁻² |
|  SNOWLMT | Height of snowfall limit above MSL | 0/1/204 | 4/101 | inst | NNB | m |





Continued on next page

Table 7.5.: *continued*

| | | | | | | |
|--|--|--------|-------|------|-----|--------------------|
|  SYNMSG_BT_CL_IR108 | Synthetic MSG SEVIRI image brightness temp. at 10.8 μ m | 3/1/14 | –/– | inst | | K |
|  SYNMSG_BT_CL_WV62 | Synthetic MSG SEVIRI image brightness temp. at 6.2 μ m | 3/1/14 | –/– | inst | | K |
|  T_2M | Temperature at 2m above ground | 0/0/0 | 103/– | inst | | K |
|  TCH | Turbulent transfer coefficient for heat and moisture (surface) | 0/0/19 | 1/– | inst | | 1 |
|  TCM | Turbulent transfer coefficient for momentum (surface) | 0/2/29 | 1/– | inst | | 1 |
|  TD_2M | Dew point temperature at 2m above ground | 0/0/6 | 103/– | inst | | K |
|  T_G | Ground temperature (temperature at sfc-atm interface) | 0/0/0 | 1/– | inst | | K |
|  T_ICE | Sea/Lake ice temperature (at ice-atm interface) | 10/2/8 | 1/– | inst | | K |
|  TMAX_2M | Maximum temperature at 2m above ground | 0/0/0 | 103/– | max | | K |
|  TMIN_2M | Minimum temperature at 2m above ground | 0/0/0 | 103/– | min | | K |
|  TOT_PREC | Total precipitation (accumulated since model start) | 0/1/52 | 1/– | accu | BCT | kg m ^{–2} |
|  TQC | Column integrated cloud water (grid scale) | 0/1/69 | 1/– | inst | | kg m ^{–2} |
|  TQI | Column integrated cloud ice (grid scale) | 0/1/70 | 1/– | inst | | kg m ^{–2} |
|  TQR | Column integrated rain (grid scale) | 0/1/45 | 1/– | inst | | kg m ^{–2} |
|  TQS | Column integrated snow (grid scale) | 0/1/46 | 1/– | inst | | kg m ^{–2} |
|  TQV | Column integrated water vapour (grid scale) | 0/1/64 | 1/– | inst | | kg m ^{–2} |
| T_S ⁵ | Temperature of the soil surface (equivalent to T_SO(0)) | 2/3/18 | 1/– | inst | | K |
|  T_SNOW | Temperature of the snow surface | 0/0/18 | 1/– | inst | | K |
|  U_10M | Zonal wind at 10m above ground | 0/2/2 | 103/– | inst | | m s ^{–1} |
|  V_10M | Meridional wind at 10m above ground | 0/2/3 | 103/– | inst | | m s ^{–1} |
|  VMAX_10M | Maximum wind at 10 m above ground | 0/2/22 | 103/– | max | | m s ^{–1} |




Continued on next page

Table 7.5.: *continued*

| | | | | | | |
|--|---|---------|-----|------|-----|--------------------|
|  W_I | Plant canopy surface water | 2/0/13 | 1/– | inst | – | kg m ⁻² |
|  W_SNOW | Snow depth water equivalent | 0/1/60 | 1/– | inst | | kg m ⁻² |
|  WW | Weather interpretation (WMO), see Table 6.8 for details. | 0/19/25 | 1/– | inst | NNB | 1 |
|  Z0 | Surface roughness (above land and water) | 2/0/1 | 1/– | inst | | m |

7.1.5. Soil-specific multi-level fields

Table 7.6.: Multi-level forecast ($VV > 0$) and initialised analysis ($VV = 0$) products of the soil model

| ShortName | Description | Discipline Category Number | Lev-Typ 1/2 | stepType | LL IntpType | Unit |
|--|--|----------------------------------|-------------|----------|-------------|--------------------|
|  T_SO | Soil temperature | 2/3/18 | 106/– | inst | | K |
|  W_SO | Soil moisture integrated over individual soil layers (ice + liquid) | 2/3/20 | 106/106 | inst | | kg m ⁻² |
|  W_SO_ICE | Soil ice content integrated over individual soil layers | 2/3/22 | 106/106 | inst | NNB | kg m ⁻² |

Soil temperature is defined at the soil depths given in Table 7.7 (column 2). Levels 1 to 8 define the full levels of the soil model. A zero gradient condition is assumed between levels 0 and 1, meaning that temperatures at the surface-atmosphere interface are set equal to the temperature at the first full level depth. (0.5 cm). Temperatures are prognosed for layers 1 to 7. At the lowermost layer (mid-level height 1458 cm) the temperature is fixed to the climatological average 2 m-temperature.

Soil moisture W_SO is prognosed for layers 1 to 6. In the two lowermost layers W_SO is filled with W_SO(6) (zero gradient condition).

⁵T_S is identical to T_SO at level 0. It will no longer be available in the future. Use T_SO(0) instead of T_S.

Table 7.7.: Soil model: vertical distribution of levels and layers

| level no. | depth [cm] | layer no. | upper/lower bounds [cm] |
|-----------|------------|-----------|-------------------------|
| 0 | 0.0 | | |
| 1 | 0.5 | 1 | 0.0 — 1.0 |
| 2 | 2.0 | 2 | 1.0 — 3.0 |
| 3 | 6.0 | 3 | 3.0 — 9.0 |
| 4 | 18.0 | 4 | 9.0 — 27.0 |
| 5 | 54.0 | 5 | 27.0 — 81.0 |
| 6 | 162.0 | 6 | 81.0 — 243.0 |
| 7 | 486.0 | 7 | 243.0 — 729.0 |
| 8 | 1458.0 | 8 | 729.0 — 2187.0 |

7.1.6. Lake-specific single-level fields

Table 7.8.: Single-level forecast ($VV > 0$) and initialised analysis ($VV = 0$) products of the lake model model on the ICON EU nest.

| ShortName | Description | Discipline Category Number | Lev-Typ 1/2 | stepType | LL IntpType | Unit |
|------------|---|----------------------------------|-------------|----------|-------------|------|
| ▣ C_T_LK | Shape factor with respect to the temperature profile in the thermocline | 1/2/10 | 162/166 | inst | – | 1 |
| ▣ H_ML_LK | Mixed-layer depth | 1/2/0 | 1/166 | inst | – | m |
| ▣ T_BOT_LK | Temperature at the water-bottom sediment interface | 1/2/1 | 162/– | inst | – | K |
| ▣ T_MNW_LK | Mean temperature of the water column | 1/2/1 | 1/162 | inst | – | K |
| ▣ T_WML_LK | Mixed-layer temperature | 1/2/1 | 1/166 | inst | – | K |

8. Output fields for soil moisture analysis SMA

The soil moisture analysis, SMA, requires the following fields from the main run at 00 UTC. They are written only by this run and from forecast hour 2 to 24. As a soil moisture analysis is made for the global and the nest domain, these fields are available for both domains, but only on the native grid.

Table 8.1.: Fields for SMA from 00 UTC run for forecast hours 2 to 24.

| ShortName | Description | Discipline Category Number | Lev-Typ 1/2 | stepType | LL IntpType | Unit |
|-----------|---------------------------------|----------------------------------|-------------|----------|-------------|-------------------|
| ALHFL_BS | Latent heat flux from bare soil | 2/0/193 | 1/- | avg | - | W m^{-2} |
| ALHFL_PL | Latent heat flux from plants | 2/0/194 | 106/106 | avg | - | W m^{-2} |
| RSTOM | Stomatal resistance | 2/0/195 | 1/- | inst | - | s m^{-1} |

The latent heat flux from plants is defined at the same soil layers as the soil moisture W_SO.

9. Extended description of available output fields

In order to facilitate the selection and interpretation of fields and to guard against possible mis-interpretation or mis-usage, the following section provides a more thorough description of the available output fields.

9.1. Cloud products

| | |
|-----------------|--|
| CLCT_MOD | Modified total cloud cover ($0 \leq \text{CLCT_MOD} \leq 1$). Used for visualization purpose (i.e. gray-scale figures) in the media. It is derived from CLC, neglecting cirrus clouds if there are only high clouds present at a given grid point. The reason for this treatment is that the general public does not regard transparent cirrus clouds as ‘real’ clouds. |
| CLDEPTH | Modified cloud depth ($0 \leq \text{CLDEPTH} \leq 1$). Used for visualization purpose (i.e. gray-scale figures) in the media. A cloud reaching a vertical extent of 700 hPa or more, has CLDEPTH= 1. |
| HBAS_CON | Height of the convective cloud base in m above msl. HBAS_CON is initialized with -500 m at points where no convection is diagnosed. |
| HTOP_CON | Same, but for cloud top. |

9.2. Atmospheric products

| | |
|----------------|--|
| HZEROCL | Height of the 0°C isotherm above MSL. At points where the temperature is below 0°C within the entire atmospheric column, HZEROCL is undefined and set to -999 . |
| SNOWLMT | Height of snow fall limit above MSL. It is defined as the height where the wet bulb temperature T_w first exceeds 1.3°C (scanning mode from top to bottom). If this threshold is never reached within the entire atmospheric column, SNOWLMT is undefined (Gridded Binary Format, 2nd edition (GRIB2) bitmap). |

9.3. Near surface products

| | |
|--------------|--|
| TD_2M | Dew point temperature at 2m above ground, i.e. the temperature to which the air must be cooled, keeping its vapour pressure e constant, such that e equals the saturation (or equilibrium) vapour pressure e_s . |
|--------------|--|

$$e_s(T_d) = e$$

| | |
|----------------|--|
| TMIN_2M | Minimum temperature at 2m above ground. Minima are collected over 6-hourly intervals on all domains. (Prior to 2015-07-07 minima were collected over 3-hourly intervals on the global grid.) |
|----------------|--|

| | |
|-----------------|---|
| TMAX_2M | Same, but for maximum 2m temperature. |
| VMAX_10M | Maximum wind gust at 10m above ground. It is diagnosed from the turbulence state in the atmospheric boundary layer, including a potential enhancement by the SSO parameterization over mountainous terrain. In the presence of deep convection, it contains an additional contribution due to convective gusts. Maxima are collected over hourly intervals on all domains. (Prior to 2015-07-07 maxima were collected over 3-hourly intervals on the global grid.) |

9.3.1. General comment on statistically processed fields

In GRIB2, the overall time interval over which a statistical process (like averaging, computation of maximum/minimum) has taken place is encoded as follows:

The beginning of the overall time interval is defined by `referenceTime + forecastTime`, whereas the end of the overall time interval is given by `referenceTime + forecastTime + lengthOfTimeRange`. See Section 10.1 for more details on statistically processed fields.

9.4. Surface products

| | |
|------------------|---|
| ASWDIFD_S | Downward solar diffuse radiation flux at the surface, averaged over forecast time. See Section 10.1 for more information on time averaging. |
| ASWDIR_S | Downward solar direct radiation flux at the surface. See Section 10.1 for more information on time averaging. |
| ALB_RAD | Ratio of upwelling to downwelling diffuse radiative flux for wavelength interval $[0.3\ \mu\text{m}, 5.0\ \mu\text{m}]$. Values over snow-free land points are based on a monthly mean MODIS climatology. MODIS values have been limited to a minimum value of 2%. |

From `ASWDIFD_S` and `ASWDIR_S` the time averaged global radiation at the surface `GLOB` can easily be computed as follows:

$$\text{GLOB} = \text{ASWDIFD_S} + \text{ASWDIR_S}$$

An estimate of `GLOB` can also be derived from the net solar radiation flux at the surface `ASOB_S` and the albedo `ALB_RAD`:

$$\text{GLOB} = \frac{\text{ASOB_S}}{1 - 0.01 \text{ALB_RAD}}$$

However be aware that this is only approximately true, because `ALB_RAD` is an instantaneous field, and it only constitutes the albedo for the diffuse component of the incoming solar radiation (“white sky” albedo). However, `ASOB_S` contains both diffuse and direct components. As a consequence, the reflection of the incoming direct radiation, which is dependent on the solar zenith angle (and described by the so called “black sky” albedo), is not correctly taken into account.

| | |
|---------------|---|
| FR_ICE | Sea and lake ice cover. This is the fraction of water covered by ice. I.e. if a grid cell contains land and water <code>FR_ICE</code> = 1 if the whole fraction of water of this grid cell is covered by ice. At lake points no fractional ice cover is allowed, meaning that <code>FR_ICE</code> is either 1 or 0. |
| H_ICE | Ice thickness over sea and frozen fresh water lakes. The maximum allowable ice thickness is limited to 3 m. New sea-ice points generated by the analysis are initialized with <code>H_ICE</code> = 0.5 m. |

| | |
|-----------------|---|
| H_SNOW | Snow depth in m. It is diagnosed from RHO_SNOW and W_SNOW according to $H_SNOW = \frac{W_SNOW}{RHO_SNOW}$ and is limited to $H_SNOW \leq 40$ m. |
| RHO_SNOW | Snow density in kg/m^3 . It can vary between 50 kg/m^3 for fresh snow and 400 kg/m^3 for compacted old snow. At snow-free points over land RHO_SNOW is set to 50 kg/m^3 , while over water it is set to 0 kg/m^3 . |
| T_ICE | Ice temperature over sea-ice and frozen lake points. Melting ice has a temperature of 273.15 K . Ice-free points over land, sea, and lakes are set to $T_SO(0)$. |
| T_G | Temperature at the atmosphere-surface interface. It is the temperature that is crucial for the computation of surface fluxes. T_G is equal to $T_SO(0)$ over open water and snow-free land. At other grid points one has <ul style="list-style-type: none"> • $T_G = T_SNOW + (1 - f_snow) * (T_SO(0) - T_SNOW)$ over (partially) snow covered grid points. f_snow is the grid point fraction that is snow covered. • $T_G = T_ICE$ over frozen sea and fresh water lakes |
| TOT_PREC | Total precipitation accumulated since model start. $TOT_PREC = RAIN_GSP + SNOW_GSP + RAIN_CON + SNOW_CON$ |
| T_SNOW | Temperature of snow surface. At snow-free points ($H_SNOW = 0$), T_SNOW contains the temperature of the soil surface $T_SO(0)$. |
| W_I | Water content of interception layer, i.e. the amount of precipitation intercepted by vegetation canopies. The maximum capacity of the interception reservoir is currently limited to $6.0E-3 \text{ kg m}^{-2}$ due to numerical reasons and thus almost negligible. Over water points, W_I is set to 0. |
| W_SNOW | Snow depth water equivalent in kg/m^2 . Set to 0 above water surfaces and snow-free land points. |
| Z0 | Surface roughness length. Constant over land, where it depends only on the type of land cover. I.e. it does not contain any contribution from subgrid-scale orography. Over water, the roughness length usually varies with time. It is computed by the so called Charnock-formula, which parameterizes the impact of waves on the roughness length. Note that this field differs significantly from the external parameter field Z0 (see Table 4.2 or 6.2). |

9.5. Soil products

| | | | | | | | | | | |
|-----------------|--|--------------|---------|---------|--------------|---------|-------------|---------|---------|--------------|
| RUNOFF_G | Water runoff from soil layers. Sum over forecast. | | | | | | | | | |
| RUNOFF_S | Surface water runoff from interception and snow reservoir and from limited infiltration rate. Sum over forecast. | | | | | | | | | |
| SOILTYP | Characterizes the dominant soiltype in a grid cell. The soiltype is assumed to be the same for all soil levels. Currently 9 soiltypes are distinguished and encoded by 1-digit integers 1-9: <table><tr><td>1: ice</td><td>2: rock</td><td>3: sand</td></tr><tr><td>4: sandyloam</td><td>5: loam</td><td>6: clayloam</td></tr><tr><td>7: clay</td><td>8: peat</td><td>9: sea water</td></tr></table> | 1: ice | 2: rock | 3: sand | 4: sandyloam | 5: loam | 6: clayloam | 7: clay | 8: peat | 9: sea water |
| 1: ice | 2: rock | 3: sand | | | | | | | | |
| 4: sandyloam | 5: loam | 6: clayloam | | | | | | | | |
| 7: clay | 8: peat | 9: sea water | | | | | | | | |

T_SO Temperature of the soil and earth surface (uppermost level). The soil full level depths at which the the soil temperature is defined are given in Table 6.10. The temperature at the uppermost level $T_SO(0)$ is not prognostic. It is rather set equal to the temperature at the first prognostic level $T_SO(1)$. The temperature at the lowermost level $T_SO(8)$ is set to the climatological 2 m temperature T_2M_CL . At sea-points, $T_SO(0:7)$ is filled with the sea-surface temperature. Note that $T_SO(0)$ does not necessarily represent the temperature at the interface soil-atmosphere. I.e. over snow/ice covered surfaces, $T_SO(0)$ represents the temperature below snow/ice.

9.6. Vertical Integrals

TQX Column integrated water species X , derived from the 3D grid-scale prognostic quantities QX , with $X \in \{V, C, I, R, S\}$. TQX is based on the assumption that there would be no sub-grid-scale variability. That assumption is particularly problematic for precipitation generation, moist turbulence and radiation.

TQX_DIA Total column integrated water species X , with $X \in \{C, I\}$. Takes into account the sub-grid-scale variability that includes simple treatments of turbulent motion and convective detrainment. These cloud variables attempt to represent all model included physical processes. They are also consistent with the cloud cover variables CLC , $CLCT$, $CLCH$, $CLCM$ and $CLCL$.

10. Remarks on statistical processing and horizontal interpolation

10.1. Statistically processed output fields

10.1.1. Time-averaged fields

The quantities

| | | | |
|---------|----------|-----------|-----------|
| ALHFL_S | ASHFL_S | AUMFL_S | AVMFL_S |
| APAB_S | ASOB_S | ASOB_T | ATHB_S |
| ATHB_T | ASWDIR_S | ASWDIFS_S | ASWDIFU_S |

constitute time averages over the respective forecast time. The averaging process is performed from forecast start ($t_0 = 0$ s) till forecast end. Thus, time averaged fields which are written to the database at $t = t_i$ contain averages for the elapsed time interval $[t_0, t_i]$.

Let Ψ denote the instantaneous value of one of the above fields. The time average $\bar{\Psi}$ at time t stored in the database is given as

$$\bar{\Psi}(t) = \frac{1}{t} \int_0^t \Psi \, dt \quad , \text{ for } t > 0.$$

For $t = 0$, the average $\bar{\Psi}$ is equal to 0. If time averages are required for other time intervals $[t_1, t_2]$, with $t_1 > 0$, these can be computed as follows:

$$\begin{aligned} \bar{\Psi}(t_2 - t_1) &= \frac{1}{t_2 - t_1} \int_{t_1}^{t_2} \Psi \, dt \\ &= \frac{1}{t_2 - t_1} \left[\int_0^{t_2} \Psi \, dt - \int_0^{t_1} \Psi \, dt \right] \\ &= \frac{1}{t_2 - t_1} [t_2 \bar{\Psi}(t_2) - t_1 \bar{\Psi}(t_1)] \end{aligned}$$

For this equation to work, it is of course necessary that the fields $\bar{\Psi}(t_1)$ and $\bar{\Psi}(t_2)$ are available from the database.

The averaging process is fully reflected by the field's GRIB2 metainfo. In order to check whether a field contains the desired time average, it is advisable to check the content of the GRIB2 keys listed in Table 10.1. I.e. `productDefinitionTemplateName=8` indicates that the field in question is statistically processed. The statistical process itself is specified by the key `typeOfStatisticalProcessing`. The averaging interval (relative to the start of the forecast) is given by

$$[\text{forecastTime}, \text{forecastTime} + \text{lengthOfTimeRange}].$$

Since the averaging process starts at $t = 0$, the key `forecastTime` is set to 0.

Table 10.1.: List of GRIB2 keys which provide information about the *averaging* process

| Octet(s) | Key | Value | Meaning |
|----------|---------------------------------|-----------------|--|
| 8-9 | productDefinitionTemplateNumber | 8 | Average, accumulation, extreme values or other statistically processed values at a horizontal level or in a horizontal layer in a continuous or non-continuous time interval |
| 19-22 | forecastTime | 0 | Starting time of the averaging process relative to the reference time. |
| 47 | typeOfStatisticalProcessing | 0 | Average |
| 50-53 | lengthOfTimeRange | <i>variable</i> | Time range over which statistical processing is done |

10.1.2. Accumulated fields

The quantities

| | | | |
|----------|----------|----------|----------|
| RAIN_GSP | SNOW_GSP | RAIN_CON | SNOW_CON |
| TOT_PREC | RUNOFF_S | RUNOFF_G | |

are accumulated over the respective forecast time. The accumulation process is performed from forecast start ($t_0 = 0$ s) till forecast end. Thus, fields which are written to the database at $t = t_i$ are accumulated for the elapsed time interval $[t_0, t_i]$.

Let Ψ denote the instantaneous value of one of the above fields. The accumulation $\hat{\Psi}$ at time t stored in the database is given as

$$\hat{\Psi}(t) = \int_0^t \Psi \, dt \quad , \text{ for } t > 0.$$

For $t = 0$, the accumulation $\hat{\Psi}$ is equal to 0. If accumulations are required for other time intervals $[t_1, t_2]$, with $t_1 > 0$, these can be computed as follows:

$$\begin{aligned}
 \hat{\Psi}(t_2 - t_1) &= \int_{t_1}^{t_2} \Psi \, dt \\
 &= \int_0^{t_2} \Psi \, dt - \int_0^{t_1} \Psi \, dt \\
 &= \hat{\Psi}(t_2) - \hat{\Psi}(t_1)
 \end{aligned}$$

For this equation to work, it is of course necessary that the fields $\hat{\Psi}(t_1)$ and $\hat{\Psi}(t_2)$ are available from the database.

The accumulation process is fully reflected by the field's GRIB2 metainfo. In order to check whether a field contains the desired accumulation, it is advisable to check the content of the GRIB2 keys listed in Table 10.2. I.e. `productDefinitionTemplateNumber=8` indicates that the field in question is statistically processed. The statistical process itself is specified by the key `typeOfStatisticalProcessing`. The accumulation interval (relative to the start of the forecast) is given by

$$[\text{forecastTime}, \text{forecastTime} + \text{lengthOfTimeRange}].$$

Since the accumulation process starts at $t = 0$, the key `forecastTime` is set to 0.

Table 10.2.: List of GRIB2 keys which provide information about the *accumulation* process

| Octet(s) | Key | Value | Meaning |
|----------|---------------------------------|----------|--|
| 8-9 | productDefinitionTemplateNumber | 8 | Average, accumulation, extreme values or other statistically processed values at a horizontal level or in a horizontal layer in a continuous or non-continuous time interval |
| 19-22 | forecastTime | 0 | Starting time of the accumulation process relative to the reference time. |
| 47 | typeOfStatisticalProcessing | 1 | Accumulation |
| 50-53 | lengthOfTimeRange | variable | Time range over which statistical processing is done |

10.1.3. Extreme value fields

The quantities

| | | |
|----------|---------|---------|
| VMAX_10M | TMAX_2M | TMIN_2M |
|----------|---------|---------|

represent extreme values, which are collected over certain time intervals χ , starting from the beginning of the forecast. The interval χ differs temperatures and gusts:

- $\chi = 6$ h for temperatures, TMAX_2M and TMIN_2M,
- $\chi = 1$ h for gusts, VMAX_10M.

After χ hours of forecast the fields are re-initialized with 0 for the first time and the next χ -hourly collection phase is started. This procedure is repeated till the end of the forecast.

Let Ψ denote the instantaneous value of one of the above fields. The maximum value Ψ_{max} at time t stored in the database is given as

$$\Psi_{max}(t) = \max(\Psi(t), \Psi_{max}(t)) \quad , \text{ for } t_i < t < t_i + \chi$$

Here, t_i indicates the time when Ψ_{max} was (re)-initialized the last time. For $t = 0$, the extreme value Ψ_{max} is equal to the instantaneous value Ψ .

Please note: Even though a 6 hour time window is used for temperatures, the database contains hourly, 2-hourly, etc. extreme temperatures. This is because the extreme temperatures are written to the database hourly, irrespective of the start/end of the 6-hourly time windows. Example: Extreme temperatures which are written into the database after a forecast time of 8 hours, contain extreme values collected over the last 2 hours. On the other hand, extreme temperatures written into the database after 12 hours contain values collected over the last 6 hours. Thus, when dealing with those fields it is very important to check the GRIB2 keys listed in Table 10.3.

productDefinitionTemplateNumber=8 indicates that the field in question is statistically processed. The statistical process itself is specified by the key typeOfStatisticalProcessing. The time interval (relative to the start of the forecast) over which the extreme value collection was performed is given by [forecastTime, forecastTime+lengthOfTimeRange]. Since the collection process is restarted every χ hours, the key forecastTime can differ from 0.

Table 10.3.: List of GRIB2 keys which provide information about the *extreme value* process

| Octet(s) | Key | Value | Meaning |
|----------|---------------------------------|-----------------|--|
| 8-9 | productDefinitionTemplateNumber | 8 | Average, accumulation, extreme values or other statistically processed values at a horizontal level or in a horizontal layer in a continuous or non-continuous time interval |
| 19-22 | forecastTime | <i>variable</i> | Starting time of the statistical process relative to the reference time. |
| 47 | typeOfStatisticalProcessing | 2,3 | Maximum/Minimum |
| 50-53 | lengthOfTimeRange | <i>variable</i> | Time range over which statistical processing is done |

10.2. Technical Details of the Horizontal Interpolation

ICON currently supports three different methods for interpolating data horizontally from the native triangular grid onto a regular lat-lon grid:

| | |
|------------|--------------------------------|
| RBF | Radial basis functions |
| BCT | Barycentric interpolation |
| NNB | Nearest-neighbor interpolation |

The interpolation selected for a particular field is indicated in the previous tables which list all available output fields.

Most of the output data on regular grids is processed using an *RBF-based interpolation method*. The algorithm approximates the input field with a linear combination of radial basis functions (RBF) located at the data sites, see, for example, [Ruppert \(2007\)](#). RBF interpolation typically produces over- and undershoots at position where the input field exhibits steep gradients. Therefore, the internal interpolation algorithm performs a cut-off by default. Note that RBF-based interpolation is *not conservative*.

Barycentric interpolation is a two-dimensional generalization of linear interpolation. This method uses just three near-neighbors to interpolate and avoids over- and undershoots, since extremal values are taken only in the data points. This interpolation makes sense for fields where the values change in a roughly piecewise linear way.

A small number of output fields is treated differently, with a *nearest-neighbor interpolation* (NNB). The nearest neighbor algorithm selects the value of the nearest point and does not consider the values of neighboring points at all, yielding a piecewise-constant interpolant.

11. ICON data in the SKY data bases of DWD

GRIB data of the numerical weather prediction models are stored in the data base SKY at DWD. Documentation on the SKY system is available in the intranet of DWD at `IT/Messnetz/Technik → Datenmanagement (technisch) → Management der DWD Fachdaten -Dokumentation → SKY`. Here, some remarks are given on the SKY categories for ICON data, and some examples are given how to retrieve data from the data base.

11.1. SKY categories for ICON

In SKY the data is stored in different categories and data base subsystems. These are identified by the `cat=CAT_NAME` parameter. The name of a category is made up of 4 parts:

\$model_\$run_\$type_\$suite

`run`, `type`, and `suite` are general for all forecast models of DWD. They can have the following values:

- **run:** **main** for main forecast runs, **ass** for assimilation runs, **pre** for pre-assimilation runs, **const** for invariant data.
- **type:** **an** for analysis data, **fc** for forecast data.
- **suite:**
 - **rout** for operational data in *db=roma*,
 - **paral** for pre-operational data in *db=parma*, or **vera** for pre-operational data in *db=vera*.
 - **exp** or **exp1** for data from experiments in *db=numex*. The category extension **exp1** is used for experiments of the NUMEX wizard, a special NUMEX user.

Data from experiments is additionally identified by the parameter *exp=NUM* where *NUM* is the experiment number.

The ICON categories start with the string **ico** for ICON data on the native ICON grid, or with **icr** for data on a regular lat-lon grid. Next follows a two-letter string to identify the domain of ICON; **gl** for the global domain, **eu** for the nest over Europe. Further particulars of the category name differ for the global and nested domain. In case of deterministic runs of the global domain, **gl** is followed by the mesh width of the model in units of 100 m, and then the number of levels preceeded by the letter **l**. As an example **icogl130l90** is on the native grid from a global model with a mesh width 13 km (grid R3B07) and 90 levels. **icrgl400l90** is data on a regular grid from a global model with mesh width 40 km (R2B06) and 90 levels. For the nested domain, the specification of the mesh width and number of levels is omitted. As an example, **icreu** is the ICON nest over Europe (with a mesh width of 6.5 km and 60 levels), interpolated to a regular lat-lon grid.

For ensemble forecasts or ensemble analyses the first part of the category is extended by an **e** (for instance **icogle** or **icrgle**). Ensemble members or ranges of ensemble members are specified by the parameter *enum=NUM* or *enum=NUM1 – NUM2* where *NUM* is the member id.

Hence, the full category name for data from a global operational forecast run of ICON on a regular grid will be **icrgl130l90_main_fc_rout**. The initial analysis for this run is in category **icogl130l90_main_an_rout**.

Since 2014-08-12 12 UTC ICON is running pre-operationally at DWD. Hence, forecast data is available in the sky database **db=parma** in categories **icogl130l90_main_fc_para** and **icrgl130l90_main_fc_para**.

Since 2015-01-20 06 UTC the *global* ICON model is running operationally at DWD. Forecast data is available in the sky database **db=roma** in categories **icogl130l90_main_fc_rout** and **icrgl130l90_main_fc_rout**.

Since 2016-01-20 06 UTC an ensemble data assimilation for ICON is running operationally at DWD. Analysis data is available in the sky database **db=roma** in the ensemble categories **icogle_main_an_rout** and **icoeue_main_an_rout**. First guess data is in **icogle_pre_fc_rout** and **icogle_pre_fc_rout**.

11.2. Retrieving ICON data from SKY

Here we shall give several examples how to retrieve ICON data from SKY. The parameter **d** specifies the reference or initial date, **s** is the forecast step, **p** the parameter, and **f** the name of the GRIB data file.

- Retrieve the 2m temperature and dew point temperature for forecast hours 3 to 78 every 3 hours of today's run at 00 UTC on the global domain from an ICON run on a R3B07 grid with 90 levels to file **icon2mdat**

```
read db=roma cat=icrgl130l90_main_fc_rout d=t00 s[h]=3/to/78/by/3 p=t_2m,td_2m bin
f=icon2mdat
```

- Retrieve the analysis of T on the native grid from yesterday 18 UTC:

```
read db=roma cat=icogl130l90_main_an_rout d=t18-1d p=T gptype=0 bin f=t_icon_ana
```

- Retrieve the 6, 12, 18, and 24 hour forecast of the 2m temperature from a forecast in experiment 10096 on 2015-09-05 at 00 UTC on the global domain from an ICON run on a R3B07 grid with 90 levels:

```
read db=numex cat=icrgl130l90_main_fc_exp exp=10096 d=2015090500 s[h]=6,12,18,24 p=
t_2m bin f=t_2m_fc.grb
```

- Retrieve accumulated precipitation of the ICON-EU nest on the regular grid every 6 hours to 72 hours from the yesterday's operational run at 12 UTC:

```
read db=roma cat=icreu_main_fc_rout d=t12-1d s[h]=6/to/72/by/6 p=tot_prec bin f=
tot_prec_ieu
```

- List the data on pressure levels of the 18 hours forecast from 06 UTC of ICON-EU nest on the regular grid. Write reference date (**d**), forecast step (**s**), level type (**lv**), value of first level (**lv1**), decoding date (**dedat**), and store date (**stdat**) in information file **icr.info**.

```
read db=roma cat=icreu_main_fc_rout d=06 step[h]=18 lv=P info=metaData metaArray=d,
s,p,lv,lv1,dedat,stdat sort=d,s,p,lv,lv1 infof=icr.info
```

- Retrieve temperature in 850 hPa from the first guess of the 40 ensemble members of the EDA on the 40 km grid in the parallel suite yesterday at 21 UTC. Sort the data by ensemble member.

```
read db=parma cat=icrgle_ass_fc_para1 enum=1/to/ d=t21-1d s=3 p=T lv=P lv1=85000
info=epsInfo sort=enum
```

- Retrieve all available time-invariant (constant) fields on the native grid and store them in the file `const_icongl`. Write reference date (d), forecast step (s), level type (lv), value of first level (lv1), decoding date (dedat), store date (stdat), and validity date (valdat) in information file `icr.info`. It is important to set **invar=true**.

```
read db=roma cat=icogl130190_const_an_rout invar=true info=metaData metaArray=d,s,p
,lv,lv1,dedat,stdat bin infof=icr.info f=const_icongl
```


A. ICON standard level heights

A.1. Level heights for zero topography height

ICON standard *half level* heights z^{h0} are listed in Table A.1. Please note that these values correspond to the actual level heights only at grid points with zero topography height, e.g. at ocean grid points.

If *full level* heights z^{f0} are required, these can be deduced as follows: Let i denote the full level index for which the height is wanted. Then the full level height z_i^{f0} is given by

$$z_i^{f0} = \frac{z_i^{h0} + z_{i+1}^{h0}}{2}.$$

See Table A.2 for a list of all full level heights of the operational setup.

A.2. Non-zero topography heights

The prerequisite "zero topography height" is seldom met in real applications. Instead the user has to compute the model level height for each grid point separately. To this end the invariant fields **HSURF** and **HHL** are provided where **HHL** is the geometric height of model half levels above sea level. The level height above ground can therefore be computed by the following formula:

$$z_i^h(x) = \text{HHL}(x) - \text{HSURF}(x)$$

$$z_i^f(x) = \frac{z_i^h(x) + z_{i+1}^h(x)}{2}$$

Table A.1.: Standard heights z_i^{h0} (i.e. for zero topography height) for all 91 vertical *half levels* of the global 13 km domain and the 61 vertical half levels for the 6.5 km EU nest.

| level index | | height | level index | | height | level index | | height |
|-------------|---------|------------|-------------|---------|------------|-------------|---------|-----------|
| global | EU nest | [m] | global | EU nest | [m] | global | EU nest | [m] |
| 1 | - | 75 000.000 | 32 | 2 | 21 569.375 | 63 | 33 | 6 621.524 |
| 2 | - | 72 363.546 | 33 | 3 | 20 731.107 | 64 | 34 | 6 221.524 |
| 3 | - | 69 842.381 | 34 | 4 | 19 942.837 | 65 | 35 | 5 821.524 |
| 4 | - | 67 357.797 | 35 | 5 | 19 201.585 | 66 | 36 | 5 421.524 |
| 5 | - | 64 946.444 | 36 | 6 | 18 504.545 | 67 | 37 | 5 033.731 |
| 6 | - | 62 606.299 | 37 | 7 | 17 849.081 | 68 | 38 | 4 659.952 |
| 7 | - | 60 335.466 | 38 | 8 | 17 232.713 | 69 | 39 | 4 300.121 |
| 8 | - | 58 132.167 | 39 | 9 | 16 653.108 | 70 | 40 | 3 954.183 |
| 9 | - | 55 976.216 | 40 | 10 | 16 108.074 | 71 | 41 | 3 622.092 |
| 10 | - | 53 877.930 | 41 | 11 | 15 595.549 | 72 | 42 | 3 303.815 |
| 11 | - | 51 824.685 | 42 | 12 | 15 113.594 | 73 | 43 | 2 999.329 |
| 12 | - | 49 826.951 | 43 | 13 | 14 660.386 | 74 | 44 | 2 708.624 |
| 13 | - | 47 890.748 | 44 | 14 | 14 234.210 | 75 | 45 | 2 431.707 |
| 14 | - | 46 014.776 | 45 | 15 | 13 821.524 | 76 | 46 | 2 168.596 |
| 15 | - | 44 197.795 | 46 | 16 | 13 421.524 | 77 | 47 | 1 919.330 |
| 16 | - | 42 438.627 | 47 | 17 | 13 021.524 | 78 | 48 | 1 683.966 |
| 17 | - | 40 736.151 | 48 | 18 | 12 621.524 | 79 | 49 | 1 462.584 |
| 18 | - | 39 089.298 | 49 | 19 | 12 221.524 | 80 | 50 | 1 255.291 |
| 19 | - | 37 497.048 | 50 | 20 | 11 821.524 | 81 | 51 | 1 062.224 |
| 20 | - | 35 958.428 | 51 | 21 | 11 421.524 | 82 | 52 | 883.557 |
| 21 | - | 34 472.507 | 52 | 22 | 11 021.524 | 83 | 53 | 719.514 |
| 22 | - | 33 038.397 | 53 | 23 | 10 621.524 | 84 | 54 | 570.373 |
| 23 | - | 31 655.249 | 54 | 24 | 10 221.524 | 85 | 55 | 436.493 |
| 24 | - | 30 322.249 | 55 | 25 | 9 821.524 | 86 | 56 | 318.336 |
| 25 | - | 29 038.622 | 56 | 26 | 9 421.524 | 87 | 57 | 216.516 |
| 26 | - | 27 803.623 | 57 | 27 | 9 021.524 | 88 | 58 | 131.880 |
| 27 | - | 26 617.350 | 58 | 28 | 8 621.524 | 89 | 59 | 65.677 |
| 28 | - | 25 488.963 | 59 | 29 | 8 221.524 | 90 | 60 | 20.000 |
| 29 | - | 24 416.908 | 60 | 30 | 7 821.524 | 91 | 61 | 0.000 |
| 30 | - | 23 408.796 | 61 | 31 | 7 421.524 | | | |
| 31 | 1 | 22 460.814 | 62 | 32 | 7 021.524 | | | |

Table A.2.: Standard heights z_i^{f0} (i.e. for zero topography height) for all 90 vertical full levels of the global 13 km domain.

| level index | height [m] | level index | height [m] | level index | height [m] |
|-------------|------------|-------------|------------|-------------|------------|
| 1 | 73 681.773 | 31 | 22 015.095 | 61 | 7 221.524 |
| 2 | 71 102.963 | 32 | 21 150.241 | 62 | 6 821.524 |
| 3 | 68 600.089 | 33 | 20 336.972 | 63 | 6 421.524 |
| 4 | 66 152.120 | 34 | 19 572.211 | 64 | 6 021.524 |
| 5 | 63 776.371 | 35 | 18 853.065 | 65 | 5 621.524 |
| 6 | 61 470.883 | 36 | 18 176.813 | 66 | 5 227.628 |
| 7 | 59 233.817 | 37 | 17 540.897 | 67 | 4 846.842 |
| 8 | 57 054.191 | 38 | 16 942.910 | 68 | 4 480.037 |
| 9 | 54 927.073 | 39 | 16 380.591 | 69 | 4 127.152 |
| 10 | 52 851.308 | 40 | 15 851.812 | 70 | 3 788.138 |
| 11 | 50 825.818 | 41 | 15 354.572 | 71 | 3 462.954 |
| 12 | 48 858.849 | 42 | 14 886.990 | 72 | 3 151.572 |
| 13 | 46 952.762 | 43 | 14 447.298 | 73 | 2 853.976 |
| 14 | 45 106.285 | 44 | 14 027.867 | 74 | 2 570.165 |
| 15 | 43 318.211 | 45 | 13 621.524 | 75 | 2 300.151 |
| 16 | 41 587.389 | 46 | 13 221.524 | 76 | 2 043.963 |
| 17 | 39 912.725 | 47 | 12 821.524 | 77 | 1 801.648 |
| 18 | 38 293.173 | 48 | 12 421.524 | 78 | 1 573.275 |
| 19 | 36 727.738 | 49 | 12 021.524 | 79 | 1 358.938 |
| 20 | 35 215.467 | 50 | 11 621.524 | 80 | 1 158.757 |
| 21 | 33 755.452 | 51 | 11 221.524 | 81 | 972.891 |
| 22 | 32 346.823 | 52 | 10 821.524 | 82 | 801.536 |
| 23 | 30 988.749 | 53 | 10 421.524 | 83 | 644.943 |
| 24 | 29 680.436 | 54 | 10 021.524 | 84 | 503.433 |
| 25 | 28 421.123 | 55 | 9 621.524 | 85 | 377.415 |
| 26 | 27 210.487 | 56 | 9 221.524 | 86 | 267.426 |
| 27 | 26 053.157 | 57 | 8 821.524 | 87 | 174.198 |
| 28 | 24 952.936 | 58 | 8 421.524 | 88 | 98.779 |
| 29 | 23 912.852 | 59 | 8 021.524 | 89 | 42.839 |
| 30 | 22 934.805 | 60 | 7 621.524 | 90 | 10.000 |

Table A.3.: Height above ground $z_i^h(x)$ (half levels) for the grid point with maximum topography height in the operational setup R03B07, 13 km spatial resolution.


| <p>Example: Height above ground HHL - HSURF</p> <p>Location with max. surface height</p> <p>CLON/CLAT = 88.180 / 27.938</p> <p>HSURF = 6425.974 m</p> | | | | | | | |
|--|------------|------------|------------|------------|------------|------------|------------|
|  | | | | | | | |
| level idx. | height [m] | level idx. | height [m] | level idx. | height [m] | level idx. | height [m] |
| 1 | 68 574.026 | 26 | 21 377.649 | 51 | 5 327.293 | 76 | 866.370 |
| 2 | 65 937.573 | 27 | 20 191.375 | 52 | 5 131.465 | 77 | 758.050 |
| 3 | 63 416.409 | 28 | 19 062.989 | 53 | 4 935.623 | 78 | 657.498 |
| 4 | 60 931.823 | 29 | 17 990.934 | 54 | 4 739.792 | 79 | 564.784 |
| 5 | 58 520.471 | 30 | 16 982.823 | 55 | 4 543.948 | 80 | 479.555 |
| 6 | 56 180.323 | 31 | 16 034.840 | 56 | 4 348.128 | 81 | 402.027 |
| 7 | 53 909.491 | 32 | 15 143.401 | 57 | 4 152.290 | 82 | 331.853 |
| 8 | 51 706.194 | 33 | 14 305.133 | 58 | 3 956.454 | 83 | 269.111 |
| 9 | 49 550.241 | 34 | 13 516.864 | 59 | 3 760.637 | 84 | 213.679 |
| 10 | 47 451.955 | 35 | 12 775.612 | 60 | 3 564.822 | 85 | 165.480 |
| 11 | 45 398.709 | 36 | 12 078.571 | 61 | 3 368.960 | 86 | 124.372 |
| 12 | 43 400.975 | 37 | 11 423.108 | 62 | 3 173.123 | 87 | 90.304 |
| 13 | 41 464.776 | 38 | 10 806.739 | 63 | 2 977.288 | 88 | 62.007 |
| 14 | 39 588.803 | 39 | 10 227.133 | 64 | 2 781.490 | 89 | 40.029 |
| 15 | 37 771.819 | 40 | 9 682.100 | 65 | 2 585.635 | 90 | 19.913 |
| 16 | 36 012.651 | 41 | 9 198.296 | 66 | 2 389.814 | 91 | 0.000 |
| 17 | 34 310.178 | 42 | 8 722.363 | 67 | 2 200.963 | | |
| 18 | 32 663.323 | 43 | 8 275.923 | 68 | 2 020.269 | | |
| 19 | 31 071.073 | 44 | 7 857.270 | 69 | 1 847.760 | | |
| 20 | 29 532.451 | 45 | 7 453.121 | 70 | 1 683.296 | | |
| 21 | 28 046.534 | 46 | 7 062.759 | 71 | 1 527.009 | | |
| 22 | 26 612.424 | 47 | 6 673.955 | 72 | 1 378.876 | | |
| 23 | 25 229.274 | 48 | 6 286.946 | 73 | 1 238.770 | | |
| 24 | 23 896.276 | 49 | 5 911.315 | 74 | 1 106.582 | | |
| 25 | 22 612.647 | 50 | 5 594.500 | 75 | 982.521 | | |

Table A.4.: Height above ground $z_i^f(x)$ (full levels) for the grid point with maximum topography height in the operational setup R03B07, 13 km spatial resolution.

Example: Height above ground, full levels

Location with max. surface height

CLON/CLAT = 88.180 / 27.938

HSURF = 6425.974 m



| level idx. | height [m] | level idx. | height [m] | level idx. | height [m] | level idx. | height [m] |
|------------|------------|------------|------------|------------|------------|------------|------------|
| 1 | 67 255.799 | 25 | 21 995.148 | 49 | 5 752.908 | 73 | 1 172.676 |
| 2 | 64 676.991 | 26 | 20 784.512 | 50 | 5 460.897 | 74 | 1 044.552 |
| 3 | 62 174.116 | 27 | 19 627.182 | 51 | 5 229.379 | 75 | 924.446 |
| 4 | 59 726.147 | 28 | 18 526.961 | 52 | 5 033.544 | 76 | 812.210 |
| 5 | 57 350.397 | 29 | 17 486.878 | 53 | 4 837.708 | 77 | 707.774 |
| 6 | 55 044.907 | 30 | 16 508.831 | 54 | 4 641.870 | 78 | 611.141 |
| 7 | 52 807.842 | 31 | 15 589.120 | 55 | 4 446.038 | 79 | 522.169 |
| 8 | 50 628.217 | 32 | 14 724.267 | 56 | 4 250.209 | 80 | 440.791 |
| 9 | 48 501.098 | 33 | 13 910.998 | 57 | 4 054.372 | 81 | 366.940 |
| 10 | 46 425.332 | 34 | 13 146.238 | 58 | 3 858.546 | 82 | 300.482 |
| 11 | 44 399.842 | 35 | 12 427.091 | 59 | 3 662.730 | 83 | 241.395 |
| 12 | 42 432.875 | 36 | 11 750.839 | 60 | 3 466.891 | 84 | 189.580 |
| 13 | 40 526.789 | 37 | 11 114.923 | 61 | 3 271.042 | 85 | 144.926 |
| 14 | 38 680.311 | 38 | 10 516.936 | 62 | 3 075.206 | 86 | 107.338 |
| 15 | 36 892.235 | 39 | 9 954.617 | 63 | 2 879.389 | 87 | 76.155 |
| 16 | 35 161.414 | 40 | 9 440.198 | 64 | 2 683.563 | 88 | 51.018 |
| 17 | 33 486.750 | 41 | 8 960.329 | 65 | 2 487.724 | 89 | 29.971 |
| 18 | 31 867.198 | 42 | 8 499.143 | 66 | 2 295.388 | 90 | 9.956 |
| 19 | 30 301.762 | 43 | 8 066.596 | 67 | 2 110.616 | | |
| 20 | 28 789.492 | 44 | 7 655.196 | 68 | 1 934.015 | | |
| 21 | 27 329.479 | 45 | 7 257.940 | 69 | 1 765.528 | | |
| 22 | 25 920.849 | 46 | 6 868.357 | 70 | 1 605.152 | | |
| 23 | 24 562.775 | 47 | 6 480.451 | 71 | 1 452.942 | | |
| 24 | 23 254.461 | 48 | 6 099.130 | 72 | 1 308.823 | | |

Bibliography

- Bloom, S. C., L. L. Takacs, A. M. D. Silva, and D. Ledvina, 1996: Data assimilation using incremental analysis updates. *Mon. Wea. Rev.*, **124**, 1256–1270.
- Leuenberger, D., M. Koller, and C. Schär, 2010: A generalization of the sleeve vertical coordinate. *Mon. Wea. Rev.*, **138**, 3683–3689.
- Polavarapu, S., S. Ren, A. M. Clayton, D. Sankey, and Y. Rochon, 2004: On the relationship between incremental analysis updating and incremental digital filtering. *Mon. Wea. Rev.*, **132**, 2495–2502.
- Ruppert, T., 2007: Diplomarbeit: Vector field reconstruction by radial basis functions. Master’s thesis, Technical University Darmstadt, Department of Mathematics.
- Wan, H., M. A. Giorgetta, G. Zängl, M. Restelli, D. Majewski, L. Bonaventura, K. Fröhlich, D. Reinert, P. Ripodas, L. Kornblueh, and J. Förstner, 2013: The ICON-1.2 hydrostatic atmospheric dynamical core on triangular grids – Part 1: Formulation and performance of the baseline version. *Geosci. Model Dev.*, **6**, 735–763.
- Zängl, G., D. Reinert, P. Ripodas, and M. Baldauf, 2015: The ICON (ICOsahedral Non-hydrostatic) modelling framework of DWD and MPI-M: Description of the non-hydrostatic dynamical core. *Q.J.R. Meteorol. Soc.*, **141**, 563–579.

Glossary

GRIB2 Gridded Binary Format, 2nd edition. [49](#)

TOA top of atmosphere. [30](#), [42](#)

WMO World Meteorological Organization. [21](#)



Deutscher Wetterdienst

Business Area "Research and Development"
Frankfurter Straße 135
63067 Offenbach
Germany